Published for SISSA by Springer

Received: April 5, 2019
Revised: June 4, 2019
Accepted: July 5, 2019
Published: July 29, 2019

Revisiting the vector leptoquark explanation of the B-physics anomalies

Claudia Cornella, Javier Fuentes-Martín and Gino Isidori

Physik-Institut, Universität Zürich,
CH-8057 Zürich, Switzerland

E-mail: claudia@physik.uzh.ch, fuentes@physik.uzh.ch, isidori@physik.uzh.ch

Abstract: We present a thorough investigation of the vector leptoquark hypothesis for a combined explanation of the B-physics anomalies. We analyze this hypothesis from a twofold perspective, taking into account recent results from B-physics observables and high-p_T searches. First, using a simplified model, we determine the general conditions for a successful low-energy fit in presence of right-handed leptoquark couplings (neglected in previous analyses). Second, we show how these conditions, in particular a sizable 2-3 family mixing, can be achieved in a motivated ultraviolet completion. Our analysis reinforces the phenomenological success of the vector leptoquark hypothesis in addressing the anomalies, and its compatibility with motivated extensions of the Standard Model based on the idea of flavor non-universal gauge interactions. The implications of right-handed leptoquark couplings for a series of key low-energy observables, namely $B_s \to \tau\tau$ and $\tau \to \mu$ lepton flavor violating processes, both in τ and in B decays, are discussed in detail. The role of the ultraviolet completion in precisely estimating other low-energy observables, most notably $\Delta F = 2$ amplitudes, is also addressed.

Keywords: Beyond Standard Model, Heavy Quark Physics

ArXiv ePrint: 1903.11517

https://doi.org/10.1007/JHEP07(2019)168

JHEP07(2019)168

Contents

JHEP07(2019)168

1 Introduction

The hints of Lepton Flavor Universality (LFU) violation in charged-current semi-leptonic $b \to c\ell\nu$ decays [1–5], as well as in $b \to s\ell\ell$ transitions [6–9], represent a very intriguing phenomenon and a fascinating challenge. Recent data confirm numerous discrepancies from the Standard Model (SM) predictions in both these sectors. Despite the fact that there is not a single measurement with a high statistical significance, and that recent data have slightly decreased the overall significance of the anomalies, the global picture is still extremely interesting: the internal consistency of available data is remarkable and, once combined, the significance of the LFU violating observables exceeds 3.7σ in $b \to s\ell\ell$ and 3.1σ in $b \to c\ell\nu$. A common origin of the two sets of anomalies is not obvious, but it is a very appealing possibility from the theoretical point of view. If confirmed as clear signals of physics beyond the Standard Model (SM), the two anomalies combined would point to non-trivial dynamics at the TeV scale, possibly linked to a solution of the SM flavor puzzle.

The initial efforts to address both sets of anomalies in terms of beyond the SM (BSM) physics have been focused on Effective Field Theory (EFT) approaches (see [10–13] for

the early attempts). However, the importance of complementing EFT approaches with appropriate simplified models with new heavy mediators was soon realized [12], and in this context leptoquark models played a key role [14–18]. Explicit heavy mediators are essential to address the compatibility of this class of SM extensions with other low-energy constraints and with high-p_T data. Due to the relatively low scale of new physics hinted at by the charged-current anomalies, high-p_T constraints are indeed quite relevant [19–27]. Given the success of some EFT approaches and simplified models in describing available data, the attention has shifted recently towards the development of more complete (and more complex) models with a consistent ultraviolet (UV) behavior (see in particular [28–42]).

Already in early attempts [11, 14], the $U_1 \sim (\mathbf{3},\mathbf{1})_{2/3}$ vector leptoquark, coupled mainly to third-generation fermions, emerged as an excellent mediator for the explanation of both sets of anomalies. The effectiveness of this state as single-mediator accounting for all available low-energy data has been established in [43]. However, the analysis of ref. [43], as most other phenomenological analyses of the U_1 leptoquark in B physics (see in particular [44–47]), is based on the simplifying hypothesis of vanishing U_1 couplings to right-handed (RH) SM fermions. This hypothesis is motivated by the absence of clear indications of non-standard RH currents in present data, and by the sake of minimality, but it does not have a strong theoretical justification. Indeed the quantum numbers of the U_1 allow for RH couplings at the renormalizable level, and in motivated UV completions such couplings naturally appear [31, 32].

The first goal of the present paper is the generalization of existing EFT/simplified-model studies on the U_1 impact in low-energy observables, taking into account non-vanishing RH couplings (mainly to the third generation). As pointed out first in [31, 32] in the context of a specific UV completion, and as we show in more general terms below, such couplings lead to a series of interesting modifications in the low-energy phenomenology compared to the pure left-handed case. We also update the analysis taking into account recent results on semileptonic B-meson decays. New data by both LHCb [8] and Belle [9] have not changed the overall significance of the anomalies in $b \to s\ell\ell$ [47–50], while preliminary data from Belle [5] have slightly decreased the significance in $b \to c\ell\nu$. However, as anticipated, the overall significance of the anomalies remains very high and the possibility of a combined explanation has become even more consistent from a theoretical point of view, due to the reduced tension with high-p_T data and other low-energy observables.

The second goal of this paper is to assess whether the conditions necessary for a successful low-energy fit to present data, compatible with high-p_T constraints [27], can be achieved in the context of a consistent UV completion of the simplified model. Here the main difficulty is to achieve a sizable 2-3 family mixing for the U_1 without introducing excessively large contributions to $\Delta F = 2$ observables from other mediators required by the consistency of the theory. As we show, this can be achieved by means of a simple extension of the scalar sector of the model originally proposed in [31] (see also [32, 37]).

We provide a detailed implementation of the U_1 leptoquark in a renormalizable model based on the (flavor non-universal) gauge group $\mathrm{SU}(4)_3 \times \mathrm{SU}(3)_{1+2} \times \mathrm{SU}(2)_L \times \mathrm{U}(1)'$, which in turn can be embedded in PS^3 [31]. In this context, we complement the simplified-model analysis by including one-loop contributions to low-energy observables (most notably

JHEP07(2019)168

$\Delta F = 2$ amplitudes and dipole operators) which can be reliably computed only within a UV-complete framework.

The paper is organized as follows. In section 2 we present the simplified-model analysis: we introduce the Lagrangian describing the U_1 couplings to SM fermions, and analyze its low-energy limit. We discuss all the observables insensitive to the UV completion (section 2.2), which are later used to fit low-energy data (section 2.3). We finally comment on the high-p_T constraints (section 2.4). The UV-complete model is presented and discussed in section 3: on the model-building side we pay particular attention to the flavor structure of the model (section 3.2); on the phenomenological side we present complete expressions for the UV-dependent (loop-induced) observables, which were omitted in the low-energy fit (section 3.3). The results are summarized in section 4.

2 The simplified U_1 model and its phenomenology

2.1 Effective interactions of the U_1 to SM fields

We consider the most general Lagrangian for the $\mathrm{SU}(2)_L$-singlet vector leptoquark, $U_1^\mu \sim (\mathbf{3},\mathbf{1})_{2/3}$, coupled to both left- and right-handed SM fields

$$\begin{aligned}\mathcal{L}_U = &-\frac{1}{2}\,U_{1\,\mu\nu}^\dagger\,U_1^{\mu\nu} + M_U^2\,U_{1\,\mu}^\dagger\,U_1^\mu - ig_c(1-\kappa_c)\,U_{1\,\mu}^\dagger\,T^a\,U_{1\,\nu}\,G^{a\,\mu\nu} \\ &- i\frac{2}{3}g_Y(1-\kappa_Y)\,U_{1\,\mu}^\dagger\,U_{1\,\nu}\,B^{\mu\nu} + (U_1^\mu J_\mu + \text{h.c.})\,,\end{aligned} \tag{2.1}$$

where $U_{1\,\mu\nu} = D_\mu U_{1\,\nu} - D_\nu U_{1\,\mu}$, with $D_\mu = \partial_\mu - ig_c\,G_\mu^a T^a - i\frac{2}{3}g_Y B_\mu$. Here G_μ^a $(a = 1,\ldots,8)$ and B_μ denote the SM $\mathrm{SU}(3)_c$ and $\mathrm{U}(1)_Y$ gauge bosons, with g_c and g_Y gauge couplings respectively, and T^a are the $\mathrm{SU}(3)_c$ generators. In models in which the vector leptoquark has a gauge origin, $\kappa_c = \kappa_Y = 0$, while this is not necessarily the case for models in which the U_1 arises as a bound state from a strongly-coupled sector. The fermion current reads[1]

$$J_\mu = \frac{g_U}{\sqrt{2}}\left[\beta_L^{i\alpha}\,(\bar{q}_L^i\gamma_\mu\ell_L^\alpha) + \beta_R^{i\alpha}\,(\bar{d}_R^i\gamma_\mu e_R^\alpha)\right]\,. \tag{2.2}$$

Here the couplings β_L and β_R are complex 3×3 matrices in flavor space. Without loss of generality, we adopt the down-quark and charged-lepton mass eigenstate basis for the $\mathrm{SU}(2)_L$ multiplets, i.e.

$$q_L^i = \begin{pmatrix} V_{ji}^*\,u_L^j \\ d_L^i \end{pmatrix}\,, \qquad \ell_L^i = \begin{pmatrix} \nu_L^i \\ e_L^i \end{pmatrix}\,. \tag{2.3}$$

In this flavor basis, we assume the following structure for the β_L and β_R couplings

$$\beta_L = \begin{pmatrix} 0 & 0 & \beta_L^{d\tau} \\ 0 & \beta_L^{s\mu} & \beta_L^{s\tau} \\ 0 & \beta_L^{b\mu} & 1 \end{pmatrix}\,, \qquad \beta_R = \begin{pmatrix} 0 & 0 & 0 \\ 0 & 0 & 0 \\ 0 & 0 & \beta_R^{b\tau} \end{pmatrix}\,, \tag{2.4}$$

[1] We ignore possible couplings to right-handed neutrinos. Such particles, if present, are assumed to be heavy enough such that they do not to play any role in low-energy observables. Vector leptoquark solutions of the B-physics anomalies involving right-handed neutrinos, light enough to fake the SM ones, have been discussed in [51, 52].

JHEP07(2019)168

where the normalization of g_U is chosen such that $\beta_L^{b\tau} = 1$. The assumed structure contains the minimal set of couplings directly connected to a combined explanation of the B-physics anomalies. The null entries in eq. (2.4) should be understood as small terms which have a negligible impact in the observables we analyze. We discuss later on the implications of this requirement on the values of $\beta_L^{d\mu}$ and $\beta_R^{b\mu}$. Under the assumption of a natural (CKM-like) flavor structure, the entries in (2.4) are expected to follow the relations $\beta_L^{d\tau},\ \beta_L^{s\mu} \ll \beta_L^{s\tau},\ \beta_L^{b\mu} \ll 1$, and $\beta_R^{b\tau} = \mathcal{O}(1)$. As we shall see, the hierarchy of the β's is well compatible and, at least in some cases, it emerges from the fit to low-energy data. The only parameter we force to be small *a priori* in the phenomenological analysis is $\beta_L^{s\tau}$, which is largely unconstrained in the simplified model (using only low-energy data) and plays a key role in setting the overall mass scale for the U_1. We set the upper limit $|\beta_L^{s\tau}| \leq 0.25$ (see section 2.3). In section 3 we show how this hierarchical structure of the β's is naturally enforced in the proposed UV completion.

By integrating out the vector leptoquark at tree level, we obtain the following high-scale ($\mu \sim M_U$) effective Lagrangian:

$$\begin{aligned}\mathcal{L}_{\text{eff}} = -\frac{2C_U}{v^2}\Big[&-2\,(\beta_L^{i\alpha})^*\beta_R^{l\beta}(\bar{\ell}_L^{\alpha}e_R^{\beta})(\bar{d}_R^{l}q_L^{i}) + \text{h.c.} + \beta_R^{i\alpha}(\beta_R^{l\beta})^*(\bar{e}_R^{\beta}\gamma_\mu e_R^{\alpha})(\bar{d}_R^{i}\gamma^\mu d_R^{l}) \\ &+ \frac{1}{2}\beta_L^{i\alpha}(\beta_L^{l\beta})^*(\bar{\ell}_L^{\beta}\gamma_\mu \ell_L^{\alpha})(\bar{q}_L^{i}\gamma^\mu q_L^{l}) + \frac{1}{2}\beta_L^{i\alpha}(\beta_L^{l\beta})^*(\bar{\ell}_L^{\beta}\sigma^a\gamma_\mu \ell_L^{\alpha})(\bar{q}_L^{i}\sigma^a\gamma^\mu q_L^{l})\Big]\,,\end{aligned} \tag{2.5}$$

where $C_U \equiv g_U^2 v^2/(4M_U^2)$ and $v = (\sqrt{2}\,G_F)^{-1/2} \approx 246\,\text{GeV}$ is the SM Higgs vacuum expectation value (vev).

2.2 The relevant low-energy observables

Since the Lagrangian in (2.1) is not renormalizable, only a limited set of low-energy observables can be reliably estimated in this setup. These are observables where the four-fermion interactions in (2.5) contribute at the tree level, or where they induce (log- or Yukawa-enhanced) loop contributions which are largely insensitive to the UV completion. In this section and in the corresponding low-energy fit we consider only such class of observables. The discussion of the UV-dependent one-loop contributions is postponed to section 3.

Taking into account these considerations, the most relevant low-energy observables can be classified as follows:

i) $\boldsymbol{b \to c(u)\tau\nu}$**.** Sizable tree-level contributions arise in the LFU ratios R_D and R_{D^*}. Due to the presence of the right-handed coupling, $\beta_R^{b\tau}$, the usual V-A contribution is supplemented by a (large) scalar contribution, yielding the following approximate expressions for R_D and R_{D^*} (see [53, 54] for the hadronic matrix elements of the scalar contribution)

$$R_D \approx R_D^{\text{SM}}\left[1 + 2C_U\,\text{Re}\left\{\left(1 - 1.5\,\eta_S\,(\beta_R^{b\tau})^*\right)\left(1 + \frac{V_{cs}}{V_{cb}}\beta_L^{s\tau} + \frac{V_{cd}}{V_{cb}}\beta_L^{d\tau}\right)\right\}\right]\,, \tag{2.6}$$

$$R_{D^*} \approx R_{D^*}^{\text{SM}}\left[1 + 2C_U\,\text{Re}\left\{\left(1 - 0.14\,\eta_S\,(\beta_R^{b\tau})^*\right)\left(1 + \frac{V_{cs}}{V_{cb}}\beta_L^{s\tau} + \frac{V_{cd}}{V_{cb}}\beta_L^{d\tau}\right)\right\}\right]\,, \tag{2.7}$$

JHEP07(2019)168

where $\eta_S \approx 1.8$ accounts for the running of the scalar operator from $M_U = 4\,\text{TeV}$ to m_b [55–57]. Interestingly, due to the scalar contribution, we obtain a significantly different scaling of the NP effect in R_D and in R_{D^*}, depending on the value of $\beta_R^{b\tau}$ (see figure 1).

Additionally, because of the chiral enhancement of the scalar contribution, large NP effects are expected in $\mathcal{B}(B_c \to \tau\nu)$

$$\mathcal{B}(B_c \to \tau\nu) = \frac{\tau_{B_c}\, m_{B_c} f_{B_c}^2 G_F^2 |V_{cb}|^2}{8\pi}\, m_\tau^2 \left(1 - \frac{m_\tau^2}{m_{B_c}^2}\right)^2 \times \left|1 + C_U \left(1 - (\beta_R^{b\tau})^* \frac{2\,\eta_S\, m_{B_c}^2}{m_\tau (m_b + m_c)}\right)\left(1 + \frac{V_{cs}}{V_{cb}}\beta_L^{s\tau} + \frac{V_{cd}}{V_{cb}}\beta_L^{d\tau}\right)\right|^2 . \tag{2.8}$$

The most stringent bounds on this observable are obtained from LEP data from which the authors of [58] obtain $\mathcal{B}(B_c \to \tau\nu) \lesssim 10\%$ (see also [59]).

Concerning the $b \to u$ transitions, the only measured observable in this category is $\mathcal{B}(B \to \tau\nu)$, for which we obtain the following expression

$$\mathcal{B}(B \to \tau\nu) = \mathcal{B}(B \to \tau\nu)_{\text{SM}} \times \left|1 + C_U \left(1 - (\beta_R^{b\tau})^* \frac{2\,\eta_S\, m_B^2}{m_\tau (m_b + m_u)}\right)\left(1 + \frac{V_{us}}{V_{ub}}\beta_L^{s\tau} + \frac{V_{ud}}{V_{ub}}\beta_L^{d\tau}\right)\right|^2 . \tag{2.9}$$

Also here, we expect large NP effects due to the chirally enhanced scalar contribution. However, in this case the connection with $R_{D^{(*)}}$ is less robust due to the possible sizable contribution from $\beta_L^{d\tau}$, which now receives a larger CKM-enhancement than the one from $\beta_L^{s\tau}$.

ii) ***b → sℓℓ.*** The vector leptoquark yields potentially large contributions to $b \to s\ell\ell$ transitions, both at tree level and at one loop. Given our assumption of vanishing couplings to electrons ($\beta_{L,R}^{qe} = 0$, for any q), tree-level contributions affect only $b \to s\mu\mu$ and $b \to s\tau\tau$ transitions along the direction $\Delta\mathcal{C}_9^{\ell\ell} = -\Delta\mathcal{C}_{10}^{\ell\ell}$ with $\ell = \mu, \tau$ (see appendix A for the Wilson coefficient definitions)

$$\Delta\mathcal{C}_9^{\ell\ell} = -\Delta\mathcal{C}_{10}^{\ell\ell} = -\frac{2\pi}{\alpha V_{tb} V_{ts}^*}\, C_U \beta_L^{s\ell} (\beta_L^{b\ell})^* . \tag{2.10}$$

Being lepton non-universal, these Wilson coefficient modifications affect the $R_{K^{(*)}}$ ratios in the following way [61, 62]

$$\begin{aligned} \Delta R_K &\equiv R_K^{[1,6]\,\text{GeV}^2} - 1 \approx 0.46\, \Delta\mathcal{C}_9^{\mu\mu} , \\ \Delta R_{K^*} &\equiv R_{K^*}^{[1.1,6]\,\text{GeV}^2} - 1 \approx 0.47\, \Delta\mathcal{C}_9^{\mu\mu} . \end{aligned} \tag{2.11}$$

As discussed in [63], a large $\beta_L^{s\tau}$ coupling can also yield a sizable lepton-universal contribution to $b \to s\ell\ell$ transitions in the $\Delta\mathcal{C}_9$ direction via a (log-enhanced) photon

JHEP07(2019)168

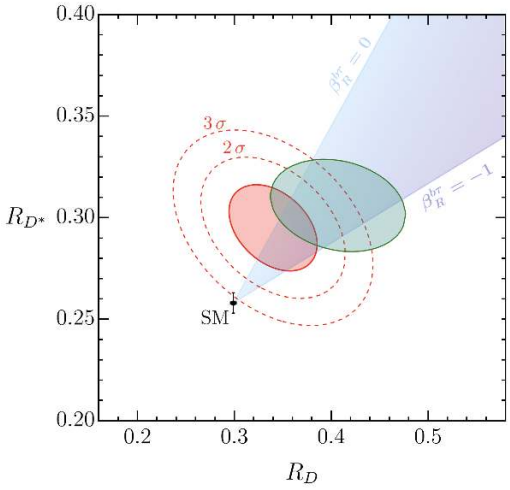

Figure 1. SU(2)$_L$-singlet vector leptoquark NP projections for R_D and R_{D^*} as a function of $\beta_R^{b\tau}$, together with the latest experimental world average (in red) and the SM prediction. For illustration, we also show the experimental 1σ HFLAV combination [60] (in green), previous to the inclusion of preliminary Belle data announced in [5].

penguin. Since the dominant contribution is given by the log-enhanced piece, it can be unambiguously recovered from the corresponding EFT computation which gives

$$\begin{aligned}\Delta\mathcal{C}_9^U &\approx -\frac{1}{V_{tb}V_{ts}^*}\frac{2}{3}C_U\sum_{\ell=e,\,\mu,\,\tau}\beta_L^{s\ell}(\beta_L^{b\ell})^*\,\log(m_b^2/M_U^2)\\ &\approx -\frac{1}{V_{tb}V_{ts}^*}\frac{2}{3}C_U\beta_L^{s\tau}(\beta_L^{b\tau})^*\,\log(m_b^2/M_U^2)\,.\end{aligned}\tag{2.12}$$

For non-zero $\beta_R^{b\mu}$, scalar-current contributions are generated in $b\to s\mu\mu$ transitions. As shown in [32], a stringent bound on $\beta_R^{b\mu}$ follows from $B_s\to\mu^+\mu^-$, since the scalar-current contribution is chirally enhanced. Fixing the other parameters to fit the current central value of $R_{K^{(*)}}$, present data imply $|\beta_R^{b\mu}|\lesssim 0.02\,|\beta_L^{b\mu}|$. Once this condition is imposed, the effect of $\beta_R^{b\mu}$ on other $b\to s\mu\mu$ observables is negligible. We can thus directly compare the corrections to $\mathcal{C}_{9,10}^{\mu\mu}$ in (2.10) and $\mathcal{C}_9^U$ in (2.12) with the global fits of these Wilson coefficients reported in [47, 48] (see also [62, 64, 65] for details on the fit methodology followed in [48]).

On the other hand, scalar currents are necessarily present in $b\to s\tau\tau$ transitions if $\beta_R^{b\tau}=\mathcal{O}(1)$. The most interesting observable in this respect is

$$\begin{aligned}\mathcal{B}(B_s\to\tau^+\tau^-) &= \mathcal{B}(B_s\to\tau^+\tau^-)_{\rm SM}\\ &\times\left[\left|1+\frac{2\pi}{\alpha V_{tb}V_{ts}^*}\frac{C_U}{C_{10}^{\rm SM}}\,\beta_L^{s\tau}\left(1-\frac{\eta_S\,m_{B_s}^2}{m_\tau(m_s+m_b)}\,(\beta_R^{b\tau})^*\right)\right|^2\right.\\ &\left.+\left(1-\frac{4m_\tau^2}{m_{B_s}^2}\right)\left|\frac{2\pi}{\alpha V_{tb}V_{ts}^*}\frac{C_U}{C_{10}^{\rm SM}}\frac{\eta_S\,m_{B_s}^2}{m_\tau(m_s+m_b)}\,\beta_L^{s\tau}(\beta_R^{b\tau})^*\right|^2\right]\,.\end{aligned}\tag{2.13}$$

JHEP07(2019)168

A milder, but still sizable, chiral enhancement occurs in $\mathcal{B}(B \to K\tau^+\tau^-)$, which can be large and within the reach of future experiments, especially for $\beta_R^{b\tau} = \mathcal{O}(1)$. Using the hadronic form factors in [66] we find

$$\begin{aligned}\mathcal{B}(B \to K\tau^+\tau^-) \approx 1.5 \cdot 10^{-7} + 10^{-3}\, C_U \left(1.4\,\mathrm{Re}\{\beta_L^{s\tau}\} - 3.3\,\mathrm{Re}\{\beta_L^{s\tau}\beta_R^{b\tau\,*}\}\right) \\ + C_U^2\,|\beta_L^{s\tau}|^2\left(3.5 - 16.4\,\mathrm{Re}\{\beta_R^{b\tau}\} + 95.0\,|\beta_R^{b\tau}|^2\right).\end{aligned} \tag{2.14}$$

An interesting feature of the vector-leptoquark solution is the absence of tree-level contributions to $b \to s\nu\nu$ observables, letting this setup easily pass the current constraints from $B \to K^{(*)}\nu\nu$.

iii) **Dipoles.** For $\beta_R^{b\tau} \neq 0$, the presence of both left- and right-handed leptoquark couplings gives rise to contributions to the radiative LFV decay $\tau \to \mu\gamma$ that are m_b-enhanced. Taking $\kappa_Y = 0$, the m_b-enhanced piece is finite and can be unambiguously computed already in the dynamical model. We find

$$\mathcal{B}(\tau \to \mu\gamma) \approx \frac{1}{\Gamma_\tau}\frac{\alpha}{64\pi^4}\frac{m_\tau^3 m_b^2}{v^4}\, C_U^2 |\beta_R^{b\tau}(\beta_L^{b\mu})^*|^2\,. \tag{2.15}$$

Analogous loop effects in the $b \to s\gamma(g)$ transitions are more sensitive to the specifics of the UV completion. Indeed the contribution proportional to the internal mass in the U_1-mediated amplitude leads to a $\mathcal{O}(m_\tau^2/m_b^2)$ suppression, rather than an enhancement, compared to the one proportional to the external mass. This latter contribution is sensitive to the details of the UV completion and cannot be reliably estimated. We thus postpone their discussion to section 3.

iv) **LFV observables.** The vector leptoquark can also yield sizable tree-level contributions to semileptonic LFV transitions. The most interesting observables are those involving the $b \to s\tau\mu$ transition. One of the observables in this category for which experimental limits are available is $B^+ \to K^+\tau\mu$. The simplified expressions are given by [32]

$$\mathcal{B}(B^+ \to K^+\tau^+\mu^-) \approx C_U^2\,|\beta_L^{s\mu}|^2\left(8.3 + 155.2\,|\beta_R^{b\tau}|^2 - 42.3\,\mathrm{Re}\{\beta_R^{b\tau}\}\right), \tag{2.16}$$

$$\mathcal{B}(B^+ \to K^+\tau^-\mu^+) \approx 8.3\, C_U^2\,|\beta_L^{b\mu}(\beta_L^{s\tau})^*|^2\,. \tag{2.17}$$

Note that, for large values of $\beta_R^{b\tau}$, the $\tau^+\mu^-$ channel is expected to yield the dominant NP contribution, provided the other couplings follow the natural flavor scaling discussed in section 2.

As in $B_s \to \tau\tau$, the NP effect in $B_s \to \tau\mu$ is chirally enhanced for $\beta_R^{b\tau} \neq 0$, making this observable of particular interest. Its expression reads

$$\begin{aligned}\mathcal{B}(B_s \to \tau^-\mu^+) = \frac{\tau_{B_s} m_{B_s} f_{B_s}^2 G_F^2}{8\pi}\, m_\tau^2\left(1 - \frac{m_\tau^2}{m_{B_s}^2}\right)^2 C_U^2 \\ \times\left|\beta_L^{s\mu}(\beta_L^{b\tau})^* - \frac{2\,\eta_S\, m_{B_s}^2}{m_\tau(m_s+m_b)}\,\beta_L^{s\mu}(\beta_R^{b\tau})^*\right|^2.\end{aligned} \tag{2.18}$$

JHEP07(2019)168

The LHCb Collaboration has recently performed the first measurement of this observable, setting the upper limit $\mathcal{B}(B_s \to \tau^\pm \mu^\pm) < 4.2 \times 10^{-5}$ at 95% C.L. [67], whose implications are discussed in the next section.

Another interesting LFV observable, relevant in the limit of large $\beta_L^{s\tau}$, is $\tau \to \mu\phi$ (see e.g. [44]). Here we find

$$\mathcal{B}(\tau \to \mu\phi) = \frac{1}{\Gamma_\tau} \frac{f_\phi^2 G_F^2}{16\pi} m_\tau^3 \left(1 - \frac{m_\phi^2}{m_\tau^2}\right)^2 \left(1 + 2\frac{m_\phi^2}{m_\tau^2}\right) C_U^2 \left|\beta_L^{s\tau} (\beta_L^{s\mu})^*\right|^2 . \tag{2.19}$$

v) **LFU in τ decays.** At the one-loop level, the effective Lagrangian in (2.5) leads to modifications of the Z and W couplings to fermions and, more generally, to LFU breaking effects in purely leptonic charged-current transitions, as extensively discussed in [68–70]. The most constraining bounds arise from LFU tests in τ decays, in particular from the ratio g_τ/g_μ. Using the results in [32], we can describe these effects via the following simplified expression

$$\left(\frac{g_\tau}{g_\mu}\right)_{\ell,\pi,K} \approx 1 - 0.08\, C_U \,, \tag{2.20}$$

where we have set $M_U = 4\,\text{TeV}$ in the evaluation of the leptoquark loop.

vi) **$\Delta F = 2$ observables.** Though important, loop contributions to $\Delta F = 2$ transitions mediated by the vector leptoquark are divergent and cannot be reliably estimated without a UV completion. The discussion of these effects is therefore postponed to section 3.3.

2.3 Fit to low-energy data

We are now ready to assess the phenomenological impact of the observables discussed in the previous section. In order to simplify the discussion we fix $\beta_R^{b\tau} = -1$. While solutions to the B-meson anomalies where $\beta_R^{b\tau} \neq -1$ are possible, and are even slightly favored by the latest data,[2] the parameter $\beta_R^{b\tau}$ is not tightly constrained and we find it useful to fix it to $\beta_R^{b\tau} = -1$ for three main reasons. First, we want to stress the main differences of this scenario with respect to the often discussed solution in which $\beta_R^{b\tau} = 0$ [43, 45, 47]. Second, this solution maximizes the NP contribution to $\Delta R_{D^{(*)}}$ (for a fixed value of g_U/M_U), allowing us to lift the NP mass spectrum, a very desirable feature in view of the tight high-p_T constraints on TeV-scale mediators. Finally, as we show in section 3, one expects $|\beta_R^{b\tau}| \approx 1$ in the explicit UV completions we are considering.

We perform a fit to low-energy data with five free parameters: C_U, $\beta_L^{d\tau}$, $\beta_L^{s\mu}$, $\beta_L^{s\tau}$, and $\beta_L^{b\mu}$.[3] The observables entering the fit, together with their SM predictions and experimental

[2] The global fits (considering only the low-energy observables in section 2.2) obtained with $\beta_R^{b\tau} = 0$ and $\beta_R^{b\tau} = -1$ differ by $\Delta\chi^2 = 1.72$, which is not statistically significant.

[3] For the CKM parameters we use the values from the NP CKM fit from UTfit [77], and PDG values [76] for the rest of the SM parameters. The presence of NP could potentially affect the extraction of these parameters from the experimental observables (see e.g. [83] for a recent discussion). However, given the flavor structure of our NP (dominantly coupled to third-generation fermions), we do not expect these modifications to significantly alter our fit results, so we neglect these corrections in the following.

JHEP07(2019)168

Observable	Experiment	Corr.	SM	U_1 expression
R_D	$0.340(30)$ [71]	-0.37	$0.299(3)$ [72–74]	(2.6)
R_{D^*}	$0.295(13)$		$0.258(5)$ [73–75]	(2.7)
$\mathcal{B}(B\to\tau\nu)$	$1.09(24)\cdot10^{-4}$ [76]	–	$0.812(54)\cdot10^{-4}$ [77]	(2.9)
$\Delta\mathcal{C}_9^{\mu\mu}=-\Delta\mathcal{C}_{10}^{\mu\mu}$	-0.40 ± 0.12 [47, 48]	-0.5	–	(2.10)
$\Delta\mathcal{C}_9^U$	-0.50 ± 0.38		–	(2.12)
$\mathcal{B}(B_s\to\tau^+\tau^-)$	$0.0(3.4)\cdot10^{-3}$ [78]	–	$7.73(49)\cdot10^{-7}$ [79]	(2.13)
$\mathcal{B}(B^+\to K^+\tau^+\tau^-)$	$1.36(0.71)\cdot10^{-3}$ [80]	–	$1.5(0.2)\cdot10^{-7}$	(2.14)
$\mathcal{B}(\tau\to\mu\gamma)$	$0.0(3.0)\cdot10^{-8}$ [60]	–	–	(2.15)
$\mathcal{B}(B^+\to K^+\tau^+\mu^-)$	$0.0(1.7)\cdot10^{-5}$ [81]	–	–	(2.16)
$\mathcal{B}(B_s\to\tau^\pm\mu^\mp)$	$0.0(2.1)\cdot10^{-5}$ [67]	–	–	(2.18)
$\mathcal{B}(\tau\to\mu\phi)$	$0.0(5.1)\cdot10^{-8}$ [82]	–	–	(2.19)
$(g_\tau/g_\mu)_{\ell,\pi,K}$	1.0000 ± 0.0014 [60]	–	1.	(2.20)

Table 1. List of observables included in the fit. The experimental values and SM predictions are also shown. The expressions of the observables in terms of the U_1 parameters are reported in section 2.2.

values, are given in table 1.[4] The vector leptoquark contributions to these observables are detailed in section 2.2. We construct the corresponding χ^2 and minimize it to obtain the best fit point and best fit regions for the model parameters. Since the observables considered in the fit are not sensitive to the individual signs of $\beta_L^{s\mu}$ and $\beta_L^{b\mu}$ but only to their product (which has to be negative), there is a degeneracy in the fit. We remove this degeneracy by considering $\beta_L^{s\mu}$ to be positive and $\beta_L^{b\mu}$ negative. We further impose $\beta_L^{s\tau}\leq 0.25$. While the latter condition is not enforced by any of the constraints considered here, it finds a natural justification in the UV-complete model discussed in section 3. As we show in this section, $\beta_L^{s\tau}$ is the breaking parameter of an approximate flavor symmetry holding at high energy and is expected to be small.

We find the following best fit 1σ regions for the fit parameters (marginalizing over the rest of parameters)

$$\begin{aligned} &C_U\in[2.8,6.4]\cdot10^{-3}\,, \qquad \beta_L^{s\tau}\in[0.15,0.25]\,, \qquad \beta_L^{d\tau}\in[-0.17,-0.02]\,,\\ &\beta_L^{b\mu}\in[-0.46,-0.16]\,, \qquad \beta_L^{s\mu}\in[0.01,0.03]\,. \end{aligned} \tag{2.21}$$

The corresponding 2D 1σ and 2σ marginalized contours are shown in figure 2. As can be seen, not all the parameters are tightly constrained. However, the 1σ regions are well

[4]The recent analyses in [47, 48] indicate a non-vanishing negative value of $\mathcal{C}_9^U$, with different levels of statistical significance. Since $\mathcal{C}_9^U$ is affected by non-factorizable hadronic contributions which are difficult to estimate precisely, we adopt the following conservative choice: our 90% C.L. upper limit on $\mathcal{C}_9^U$ is set to 0, while the 90% C.L. lower limit is set to -1.0 (which coincides with the 90% C.L. lower limit in [48]). This way the central value of $\mathcal{C}_9^U$ is closer to the value quoted in [47], but the error is ~ 1.5 times larger.

JHEP07(2019)168

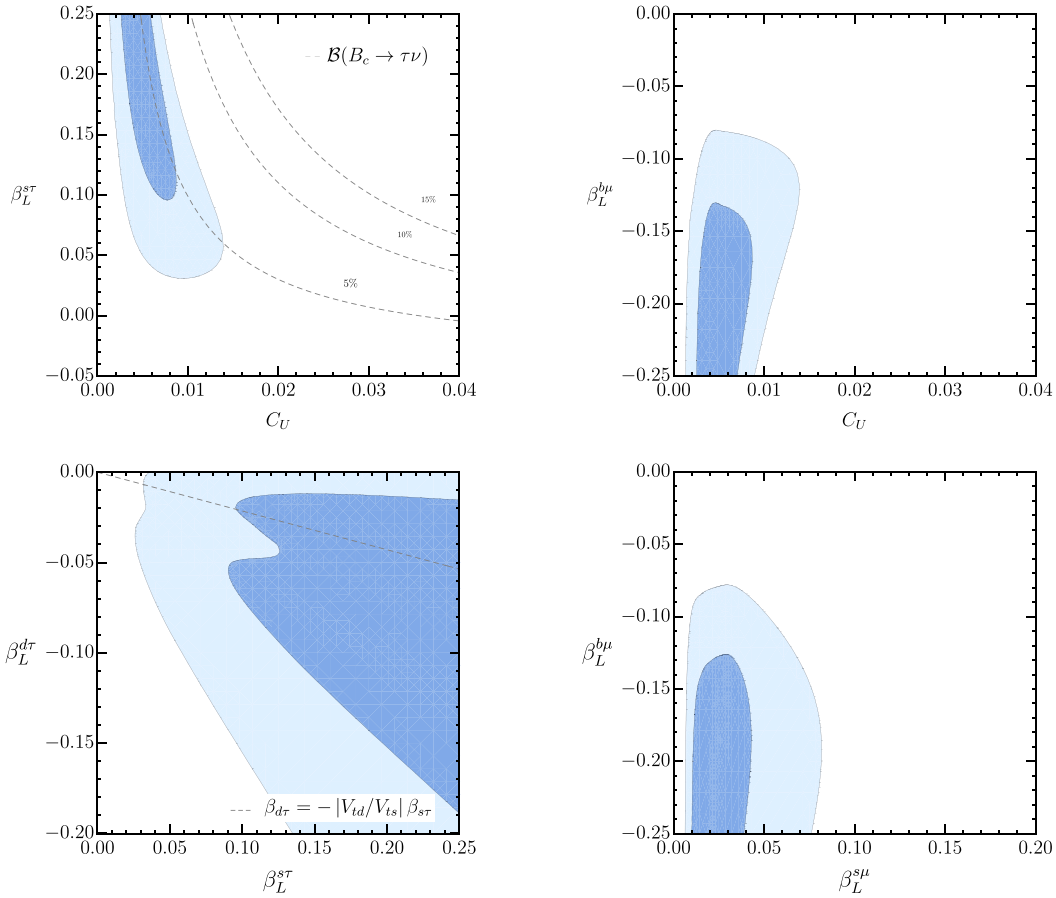

Figure 2. Preferred 2D regions from the fit, marginalizing over the rest of the parameters. The $\Delta\chi^2 \leq 2.30$ (1σ) and $\Delta\chi^2 \leq 6.18$ (2σ) regions are shown in blue and light blue, respectively. Dashed isolines for $\mathcal{B}(B_c \to \tau\nu)$ assuming $R_{D^{(*)}}$ to be fixed to their current experimental central values are also shown.

compatible with the expected hierarchical structure of the β's. More precisely, data are compatible with $|\beta_L^{s\tau}|,\ |\beta_L^{b\mu}| = O(10\%)$ and $|\beta_L^{d\tau}|,\ |\beta_L^{s\mu}| = \text{few} \times 10^{-2}$.

The main conclusions we can draw from this fit are the following:

- $\Delta R_{D^{(*)}}$ fixes the product of C_U and $\beta_L^{s\tau}$, and the two are therefore anticorrelated, see figure 2 (top left). The same behavior is also seen in the pure left-handed scenario [43]. However, in this case the presence of the right-handed coupling yields a significantly larger NP contribution to ΔR_D for fixed C_U, allowing for smaller values of C_U, or equivalently for a larger M_U at fixed vector leptoquark coupling g_U. The impact of this concerning high-p_T searches is discussed in section 2.4. As shown in [32], the low-region of $\beta_L^{s\tau}$, with correspondingly larger values of C_U, receives important constraints from $\tau \to \mu\gamma$, which sets an upper limit in C_U of about 0.02. On the other hand, we find that the radiative constraints from LFU ratios in τ decays give comparable limits to those from $\tau \to \mu\gamma$.

JHEP07(2019)168

- Given the sizable values of $\beta_L^{s\tau}$ and the chiral enhancement due to $\beta_R^{b\tau}$, we end up with an $\mathcal{O}(10^3)$ NP enhancement in $\mathcal{B}(B_s \to \tau^+\tau^-)$ and in $\mathcal{B}(B \to K\tau^+\tau^-)$, within the reach of future experimental limits, see figure 3 (bottom left). Improvements in these observables are therefore crucial to test the validity of this setup.

- A similar scalar enhancement could also yield dangerous NP effects in $\mathcal{B}(B \to \tau\nu)$. Those are however alleviated in the presence of $\beta_L^{d\tau}$, see figure 2 (bottom left). In particular, while a zero value for $\beta_L^{d\tau}$ is disfavored in our setup, a wide range of non-zero values for $\beta_L^{d\tau}$ are allowed. Interestingly, the relation $\beta_L^{d\tau} = -|V_{td}/V_{ts}|\,\beta_L^{s\tau}$, which is naturally expected in a U(2) framework with a single spurion breaking [43], is perfectly consistent with our preferred fit region. This relation arises naturally also in the UV completion given in section 3.

- As in the pure left-handed case, the couplings $\beta_L^{b\mu}$ and $\beta_L^{s\mu}$ are anticorrelated and need to be of opposite sign in order to reproduce the measured value of $\Delta C_9^{\mu\mu} = -\Delta C_{10}^{\mu\mu}$, see figure 2 (bottom right). The maximum size of $\beta_L^{s\mu}$ is mildly constrained by the current experimental bound in $\mathcal{B}(B^+ \to K^+\tau\mu)$. More stringent constraints are obtained by the recent LHCb measurement of $\mathcal{B}(B_s \to \tau\mu)$, for which larger NP effects are expected due to the additional chiral enhancement. On the other hand, the maximum size of $\beta_L^{b\mu}$ is bounded by the constraints from $\tau \to \mu\gamma$. Finally, NP contributions to $\tau \to \mu\phi$ are limited by our assumption $\beta_L^{s\tau} \leq 0.25$. We find these contributions to be more than two orders of magnitude below the current experimental limits, see figure 3 (bottom right).

- The universal contribution along the $\Delta\mathcal{C}_9$ direction is correlated with the NP effect in $R_{D^{(*)}}$. Marginalizing over all other parameters, we find the best fit 1σ region $\Delta\mathcal{C}_9^U \in [-0.33, -0.19]$, in reasonable agreement with what is expected from the fit to $b \to s\mu\mu$ observables [47, 48].

The best fit region in the proposed framework is consistent with a combined explanation of the two LFU anomalies. This is illustrated in figure 3 (top left) where we show the 1σ and 2σ preferred fit regions for $\Delta R_{K^{(*)}}$ and $\Delta R_{D^{(*)}}$ ($\Delta R_{D^{(*)}} \equiv R_{D^{(*)}}/R_{D^{(*)}}^{\rm SM} - 1$), together with their experimental values. Moreover, our setup predicts interesting implications that connect the NP contributions to the anomalies with other observables. The most remarkable of those involves large (chirally enhanced) NP effects in LFV and in $b \to s\tau\tau$ transitions. As shown in figure 3, the model predictions for several observables concerning these transitions, such as $\tau \to \mu\gamma$, $B \to K\tau\mu$ or $B_s \to \tau\tau$, lie close to the current experimental limits.

2.4 Constraints from high-p_T observables

Having analyzed the low-energy constraints on the dynamical model introduced in section 2, we comment now on the most relevant high-p_T constraints on this setup (with the couplings fixed by the fit presented above). To this purpose, we take advantage of the recent analysis in [27], where the high-p_T constraints on a SU(2)$_L$-singlet vector leptoquark have been

JHEP07(2019)168

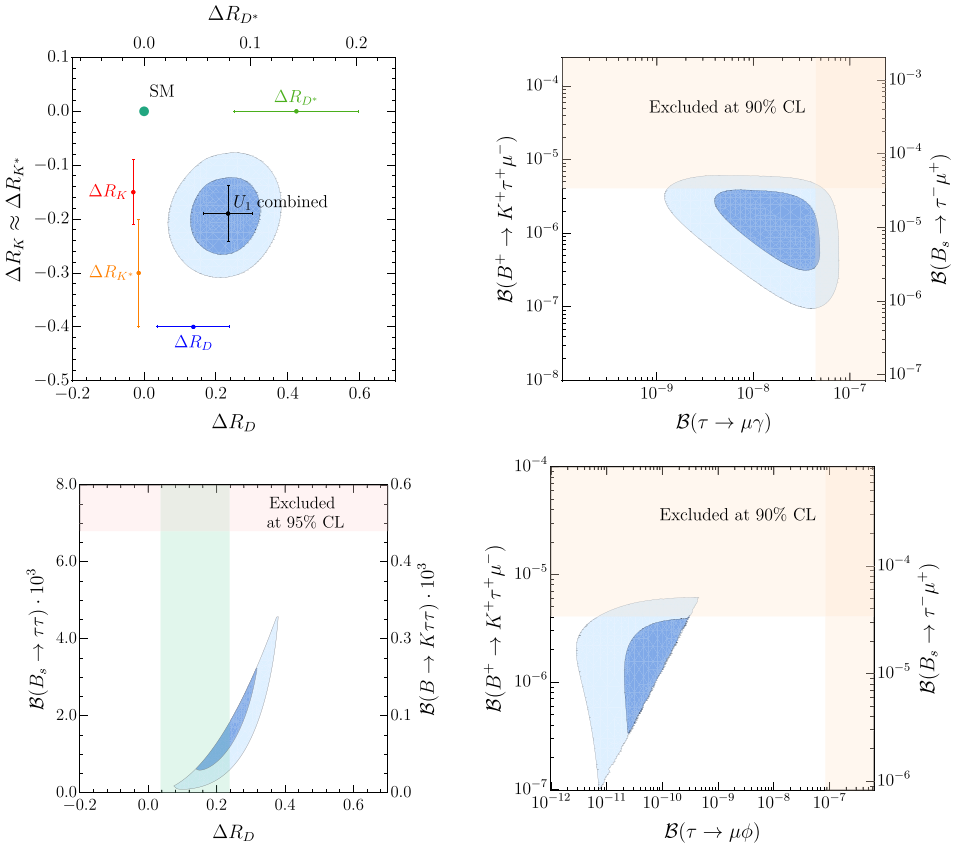

Figure 3. Preferred 2D fit regions for different experimental observables, marginalizing over the rest of parameters. The $\Delta\chi^2 \leq 2.30$ (1σ) and $\Delta\chi^2 \leq 6.18$ (2σ) regions are shown in blue and light blue, respectively. The intervals in the top left plot show the current experimental measurements of $\Delta R_{K^{(*)}}$ and $\Delta R_{D^{(*)}}$ with 1σ errors. The cross corresponds to the combination of these measurements assuming the relation among these observables in our U_1 model. The red (orange) bands show the 95% (90%) CL experimental exclusion limits, while the green band indicates the experimental measurement at 1σ.

analyzed in general terms. Similarly to the previous section, we fix $\beta_R^{b\tau} = -1$ and comment on the main differences with respect to the chiral vector leptoquark solution ($\beta_R^{b\tau} = 0$).

One of the most relevant collider signatures of the model is the production of tau lepton pairs at high energies ($pp \to \tau\tau + X$) via a tree-level t-channel leptoquark exchange. The dominant production mechanism for this channel is through the $b\bar{b}$ initial state. Though slightly pdf enhanced, the production via $b\bar{s}$ or $s\bar{s}$ are suppressed by $\beta_L^{s\tau}$. Due to the smallness of this coupling resulting from the low-energy fit, these latter contributions only give a small correction. The most stringent limits in the ditau search are provided by the ATLAS Collaboration with 36.1 fb^{-1} of 13 TeV data [84]. A recast of the ATLAS search [27] shows that a significant region of the parameter space (corresponding to values of $\beta_L^{s\tau} \lesssim 0.08\,(0.03)$ for the 1σ (2σ) fit regions) is already excluded by this search, see figure 2. However, a large portion of the parameter space remains viable. In figure 4 we present the current limits, and those obtained by extrapolating the statistics to 3 ab^{-1},

JHEP07(2019)168

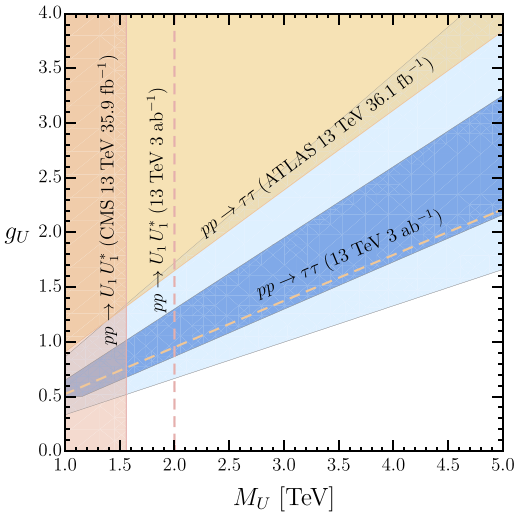

Figure 4. High-p_T constraints on the SU(2)$_L$-singlet vector leptoquark model with $\beta_R^{b\tau} = -1$. The 1σ and 2σ regions preferred by the low-energy fit are shown in blue and light blue, respectively.

assuming that no NP signal will show up and that the SM background uncertainties scale with luminosity as $1/\sqrt{N}$. Interestingly, and in contrast with the chiral vector leptoquark solution (see e.g. [25, 45]), the preferred parameter space of the scenario we propose will be almost fully probed by the HL-LHC, provided the current central value for the $R_{D^{(*)}}$ anomaly stays unchanged. This difference is due to the additional contributions from $b_R b_R \to \tau_R \tau_R$ and $b_R b_L \to \tau_R \tau_L$ when $\beta_R^{b\tau} = -1$, which are not fully compensated by the increased NP scale due to the additional scalar contribution in $R_{D^{(*)}}$. Analogous limits from $pp \to \tau\mu$ or $pp \to \mu\mu$ are found to be weaker, due to the smallness of $\beta_L^{b\mu}$ and $\beta_L^{s\mu}$, and thus do not play any role in the present discussion [27]. Similarly, and in close analogy to what happens in the chiral leptoquark case [26], the corresponding limits from $pp \to \tau\nu$ are also weaker than the ones from $pp \to \tau\tau$ [27]. This is due to the smallness of $V_{cs}^* \beta_L^{s\tau}$ and $V_{cb}^* \beta_L^{b\tau}$, in the present model, compared to $\beta_L^{b\tau}$.

Complementary constraints can be obtained from bounds on leptoquark pair production, i.e. $pp \to U_1 U_1^*$. Being charged under color, leptoquark pair production is dominated by QCD and therefore it is (almost) independent of the g_U coupling. In our case (with $\beta_R^{b\tau} = -1$), the dominant decay channel of the vector leptoquark is through a b-quark and a τ-lepton. The CMS Collaboration has performed a search on $pp \to \tau\tau jj$ with 35.9 fb^{-1} of data 13 TeV [85]. Recasting the CMS search one obtains a lower limit in the leptoquark mass of $M_U \gtrsim 1.5$ TeV [27]. As in the case of $pp \to \tau\tau$ limits, in figure 4 we report both present and HL-LHC (3 ab^{-1}) projections for the pair-production limits.

3 A possible UV completion

An important limitation of the phenomenological analysis in section 2 is the inability to reliably estimate some of the loop contributions that are potentially relevant for the low-energy phenomenology. Moreover, it is not obvious whether the conditions necessary for a

JHEP07(2019)168

successful low-energy fit, and the compatibility with high-p_T constraints, can be achieved in the context of a consistent UV complete model. For instance, the non-vanishing value of $\beta_L^{s\tau}$ required by the fit is incompatible with the UV model proposed in [31], and even assuming such a large off-diagonal flavor coupling can be generated (via a suitable modification of the model), it is not clear if the resulting B_s-mixing amplitude is in agreement with data. Furthermore, UV-complete models necessarily introduce new particles other than the U_1, which could alter the conclusions based on the U_1 alone.

We address these questions in this section. To this purpose, we introduce a specific , but sufficiently general, UV-complete model that allows us to reproduce all the features of the simplified Lagrangian in (2.1).

3.1 Gauge symmetry and matter content

The model we propose is based on the so-called "4321" gauge group, $\mathcal{G}_{4321} \equiv \mathrm{SU}(4) \times \mathrm{SU}(3)' \times \mathrm{SU}(2)_L \times \mathrm{U}(1)'$ which contains the SM gauge group as a subgroup.[5] We denote the corresponding gauge fields as H_μ^α, C_μ^a, W_μ^i and B'_μ, the gauge couplings as g_4, g_3, g_L, g_1, and the generators as T_4^α, T_3^a, T_L^i and Y', with indices $\alpha = 1, \ldots, 15$, $a = 1, \ldots, 8$ and $i = 1, 2, 3$. We normalize the generators so that $\mathrm{Tr}(T^A T^B) = \delta_{AB}$. Many models based in this gauge symmetry have been proposed in the recent literature, see e.g. [22, 28, 38, 86]. In contrast to these proposals, in our model the gauge group is non-universal among the different SM-like families. This (flavored) gauge structure, which can be regarded as a low-energy limit of the PS^3 model proposed in [31] (see also [32, 37]), also yields interesting implications in the Yukawa sector of the theory, hinting to a possible explanation of the SM flavor hierarchies.

The matter content of the theory, together with its representation under $\mathcal{G}_{4321}$, is given in table 2. The discussion on the neutrino sector of the theory is beyond the scope of this paper. The observed neutrino masses and mixing angles can be reproduced, without fine-tuning, via an inverse see-saw mechanism by adding additional gauge-singlet fermions [37] (see also [87] for a similar implementation). The fermion content of the model comprises three SM-like and two vector-like families. Two of the SM-like families are singlets under the SU(4) gauge group: q'^i_L, u'^i_R, d'^i_R, ℓ'^i_L and e'^i_R, with $i = 1, 2$. The third family SM-like fermions form SU(4) multiplets, $\psi_{L,u,d}$, in which quarks and leptons are unified as $\psi'^\intercal_L \equiv (q'^3_L \;\; \ell'^3_L)$, $\psi'^\intercal_u \equiv (u'^3_R \;\; \nu'^3_R)$ and $\psi'^\intercal_d \equiv (d'^3_R \;\; e'^3_L)$. The vector-like families, $\chi^i_{L,R}$ $(i = 1, 2)$, also form SU(4) multiplets, which decompose under the SM gauge group as $\chi^{i\,\intercal}_{L,R} \equiv (Q'^i_{L,R}, L'^i_{L,R})$, where $Q'^i_{L,R}$ and $L'^i_{L,R}$ have the same quantum numbers as the SM $\mathrm{SU}(2)_L$ doublets.

The spontaneous symmetry breaking (SSB) of the "4321" gauge group down to the SM one is triggered by the vev of $\Omega_{1,3,15}$. While only Ω_3 is enough to trigger the desired symmetry breaking pattern, the additional scalar fields are needed to generate the correct fermion-mixing effects, see section 3.2. An important difference with respect to the models in [31, 32, 37] is given by the presence of an additional scalar field, Ω_{15}. As we show in the next section, this field plays a key role in generating the 2-3 flavor misalignment in the

[5] As argued in [27], this is the minimal gauge group containing the U_1 as a gauge boson which fulfills the necessary requirements to provide a successful explanation of the anomalies while remaining consistent with high-p_T data. See also [28] for the first "4321" implementation aimed to address the B-anomalies, where this point was also noted.

JHEP07(2019)168

Field	SU(4)	SU(3)′	SU(2)$_L$	U(1)′
q'^i_L	**1**	**3**	**2**	1/6
u'^i_R	**1**	**3**	**1**	2/3
d'^i_R	**1**	**3**	**1**	−1/3
ℓ'^i_L	**1**	**1**	**2**	−1/2
e'^i_R	**1**	**1**	**1**	−1
ψ'_L	**4**	**1**	**2**	0
ψ'_u	**4**	**1**	**1**	1/2
ψ'_d	**4**	**1**	**1**	−1/2
χ^i_L	**4**	**1**	**2**	0
χ^i_R	**4**	**1**	**2**	0
H_1	**1**	**1**	**2**	1/2
H_{15}	**15**	**1**	**2**	1/2
Ω_1	$\bar{\mathbf{4}}$	**1**	**1**	−1/2
Ω_3	$\bar{\mathbf{4}}$	**3**	**1**	1/6
Ω_{15}	**15**	**1**	**1**	0

Table 2. Field content of the model ($i = 1, 2$). Particles added to the SM matter content are shown on a grey background.

U_1 interactions required by the low-energy fit, see figure 2 (top left). We assume that the scalar potential is such that these scalar fields develop vevs in the following directions

$$\langle \Omega_1^{\mathsf{T}} \rangle = \frac{1}{\sqrt{2}} \begin{pmatrix} 0 \\ 0 \\ 0 \\ \omega_1 \end{pmatrix}, \quad \langle \Omega_3^{\mathsf{T}} \rangle = \frac{1}{\sqrt{2}} \begin{pmatrix} \omega_3 & 0 & 0 \\ 0 & \omega_3 & 0 \\ 0 & 0 & \omega_3 \\ 0 & 0 & 0 \end{pmatrix}, \quad \langle \Omega_{15} \rangle = \omega_{15}\, T_4^{15}\,, \tag{3.1}$$

with $\omega_{1,3,15} = \mathcal{O}(\text{TeV})$. These scalar fields can be decomposed under the unbroken SM subgroup as $\Omega_1 \sim (\bar{\mathbf{3}}, \mathbf{1})_{-2/3} \oplus (\mathbf{1}, \mathbf{1})_0$, $\Omega_3 \sim (\mathbf{8}, \mathbf{1})_0 \oplus (\mathbf{3}, \mathbf{1})_{2/3} \oplus (\mathbf{1}, \mathbf{1})_0$, and $\Omega_{15} \sim (\mathbf{8}, \mathbf{1})_0 \oplus (\mathbf{3}, \mathbf{1})_{2/3} \oplus (\mathbf{1}, \mathbf{1})_0$. As a result, after removing the Goldstones, we end up with two real color octects, two real and one complex singlets, and two complex leptoquarks. The vector-boson spectrum after SSB, which coincides with the one originally proposed in ref. [28], contains the following massive fields

$$\begin{aligned} U_\mu^{1,2,3} &= \frac{1}{\sqrt{2}} \left(H_\mu^{9,11,13} - i H_\mu^{10,12,14} \right), \quad Z'_\mu = \frac{1}{\sqrt{g_4^2 + \frac{2}{3} g_1^2}} \left(g_4 H_\mu^{15} - \sqrt{\frac{2}{3}}\, g_1 B'_\mu \right), \\ G'^a_\mu &= \frac{1}{\sqrt{g_4^2 + g_3^2}} \left(g_4\, H_\mu^a - g_3\, C_\mu^a \right), \end{aligned} \tag{3.2}$$

JHEP07(2019)168

whose masses read [34]

$$M_U = \frac{1}{2} g_4 \sqrt{\omega_1^2 + \omega_3^2 + \frac{4}{3}\omega_{15}^2}\,, \quad M_{Z'} = \frac{1}{2}\sqrt{\frac{3}{2}g_4^2 + g_1^2}\sqrt{\omega_1^2 + \frac{1}{2}\omega_3^2}\,, \quad M_{G'} = \sqrt{\frac{g_4^2 + g_3^2}{2}}\,\omega_3\,. \tag{3.3}$$

The orthogonal combinations to G'^a_μ and Z'_μ correspond to the SM gauge fields G^a_μ and B_μ, whose couplings are $g_c = g_3 g_4/\sqrt{g_4^2 + g_3^2}$ and $g_Y = g_1 g_4/\sqrt{g_4^2 + \frac{2}{3}\,g_1^2}$. In particular, the SM color group corresponds to $\mathrm{SU}(3)_c \equiv [\mathrm{SU}(3)_4 \times \mathrm{SU}(3)']_{\rm diag}$ and $\mathrm{U}(1)_Y \equiv [\mathrm{U}(1)_4 \times \mathrm{U}(1)']_{\rm diag}$, with $\mathrm{SU}(3)_4 \times \mathrm{U}(1)_4 \subset \mathrm{SU}(4)$. In turn, hypercharge is given in terms of the original gauge generators and $\mathrm{U}(1)'$-charges by $Y = \sqrt{2/3}\,T_4^{15} + Y'$. The SU(2) group remains unaffected and directly corresponds to the SM $\mathrm{SU}(2)_L$.

The two remaining scalar fields, $H_{1,15}$, are responsible of electroweak symmetry breaking (EWSB). The H_{15} field decomposes under the SM gauge group as $H_{15} \sim (\mathbf{8},\mathbf{2})_{1/2} \oplus (\mathbf{3},\mathbf{2})_{7/6} \oplus (\bar{\mathbf{3}},\mathbf{2})_{-1/6} \oplus (\mathbf{1},\mathbf{2})_{1/2}$, and therefore contains a Higgs doublet which we denote by H_{15}^0. This additional Higgs field is needed to generate a (small) splitting between the quark and lepton masses of the would-be third family. We assume that the scalar potential is such that only H_1 and H_{15}^0 acquire a vev around the electroweak scale. Namely, $|\langle H_1\rangle| = v_1/\sqrt{2}$ and $|\langle H_{15}^0\rangle| = v_{15}/\sqrt{2}$, with the SM vev being given by $v = \sqrt{v_1^2 + v_{15}^2}$.

The leptoquarks in the model do not mediate proton decay at the renormalizable level since they do not couple to quark pairs. As in the SM, baryon and lepton number arise as accidental global symmetries and proton decay can only happen at the level of dimension-six (or higher) operators.

3.2 Flavor symmetries and fermion-mixing structure

In the absence of vector-like fermions, only $\psi'_{L,u,d}$, which we identify with the would-be third family, couple to the U_1. As required by gauge anomaly cancellation, both left- and right-handed fermions need to be charged under SU(4), thus the U_1 couples to both fermion chiralities with the same coupling strength. The other two SM-like families, being SU(4) singlets, couple to the Z' and G' but not to the U_1. We therefore have

$$\mathcal{L}_U \supset \frac{g_4}{\sqrt{2}}\, U_1^\mu \left[\beta'_L\,(\bar\Psi'_q \gamma_\mu P_L \Psi'_\ell) + \beta'_u\,(\bar u'_R \gamma_\mu \nu'_R) + \beta'_d\,(\bar d'_R \gamma_\mu e'_R) + (\bar Q'^i_R \gamma_\mu L'^i_R)\right] + \text{h.c.}\,, \tag{3.4}$$

where $\Psi_q^\intercal = (q'^1_L\ q'^2_L\ q'^3_L\ Q'^1_L\ Q'^2_L)$, $\Psi_\ell^\intercal = (\ell'^1_L\ \ell'^2_L\ \ell'^3_L\ L'^1_L\ L'^2_L)$, $\beta'_L = \mathrm{diag}(0,0,1,1,1)$, $\beta'_{u,d} = \mathrm{diag}(0,0,1)$. This is a good starting point to reproduce the solution found in section 2. Subleading couplings to the light generations can then be induced via mass-mixing with the two vector-like families. Given our choice of quantum numbers for the vector-like fermions, mixing effects can only appear in the left-handed sector (before EWSB). In what follows we discuss these effects, paying special attention to the flavor symmetries of the model.

In the absence of Yukawa interactions, the fermion sector of the model has the accidental flavor symmetry

$$\mathcal{G}_F \equiv \mathrm{U}(2)_q \times \mathrm{U}(2)_{u_R} \times \mathrm{U}(2)_{d_R} \times \mathrm{U}(2)_\ell \times \mathrm{U}(2)_{e_R} \times \mathrm{U}(1)_{\psi_u} \times \mathrm{U}(1)_{\psi_d} \times \mathrm{U}(3)_{\psi_L + \chi_L} \times \mathrm{U}(2)_{\chi_R}\,. \tag{3.5}$$

JHEP07(2019)168

We assume that $\mathrm{U}(3)_{\psi_L+\chi_L} \times \mathrm{U}(2)_{\chi_R}$ is explicitly broken to $\mathrm{U}(2)_\chi \times \mathrm{U}(1)_{\psi_L}$, where $\mathrm{U}(2)_\chi \equiv \mathrm{U}(2)_{\chi_L+\chi_R}$, by the vector-like mass term. In other words, we assume that the vector-like mass term for χ is proportional to the identity matrix. While departures from this assumption are possible, $\mathrm{U}(2)_\chi$-breaking terms are severely constrained, in our model, by $\Delta F = 2$ observables. We therefore stick to this assumption for simplicity and consider possible $\mathrm{U}(2)_\chi$-breaking terms as small perturbations around this solution. The remaining flavor symmetry is explicitly broken by the (renormalizable) Yukawa interactions. Let us analyze these interactions separately.

We focus first on the Yukawa terms involving the $\Omega_{1,3}$ fields. Without loss of generality, we can use the remaining flavor symmetry to rotate to a basis in which these interactions take the form

$$-\mathcal{L} \supset M_\chi\, \bar{\chi}_L\, \chi_R + \hat{\lambda}_q\, \bar{q}_L \Omega_3 \chi_R + \hat{\lambda}_\ell\, W\, \bar{\ell}_L \Omega_1 \chi_R + \text{h.c.}\,, \tag{3.6}$$

where M_χ is a (flavor-universal) mass term and W, $\hat{\lambda}_q$ and $\hat{\lambda}_\ell$ are 2×2 matrices in flavor space, with $\hat{\lambda}_{q,\ell}$ diagonal and W unitary. After SSB, these terms induce a mass-mixing between the vector-like and the first- and second-generation SM-like fermions. This way we effectively introduce (small) couplings between the new vectors and the light-generation fermions. We parametrize $\hat{\lambda}_{q,\ell}$ as follows

$$\begin{aligned} \hat{\lambda}_q &= \mathrm{diag}(\lambda_q + \delta\lambda_q,\, \lambda_q)\,, \\ \hat{\lambda}_\ell &= \mathrm{diag}(\delta\lambda_\ell,\, \lambda_\ell)\,. \end{aligned} \tag{3.7}$$

If considered separately, the parameters $\lambda_{q,\ell}$ yield the following explicit breaking of the flavor symmetry

$$\begin{aligned} &\mathrm{U}(2)_q \times \mathrm{U}(2)_\chi \xrightarrow{\lambda_q} \mathrm{U}(2)_{q+\chi}\,, \\ &\mathrm{U}(2)_\ell \times \mathrm{U}(2)_\chi \xrightarrow{\lambda_\ell} \mathrm{U}(1)_{\ell_1} \times \mathrm{U}(1)_{\chi_1} \times \mathrm{U}(1)_{\ell_2+\chi_2}\,. \end{aligned} \tag{3.8}$$

The parameter $\delta\lambda_q$ denotes a possible sub-leading term (i.e. $\delta\lambda_q \ll \lambda_q$) that introduces a small explicit breaking of the $\mathrm{U}(2)_{q+\chi}$ symmetry, and is tightly constrained by $\Delta F = 2$ observables. Similarly, $\delta\lambda_\ell$ corresponds to a possible sub-leading term (i.e. $\delta\lambda_\ell \ll \lambda_\ell$) that explicitly breaks the $\mathrm{U}(1)_{\ell_1} \times \mathrm{U}(1)_{\chi_1}$ symmetry, and is constrained by LFV observables such as $K_L \to \mu e$. The simultaneous presence of λ_q and λ_ℓ yields the collective breaking of $\mathrm{U}(2)_q \times \mathrm{U}(2)_\ell \times \mathrm{U}(2)_\chi$. However, since both couplings are required for this breaking to take place, the full breaking of the flavor symmetry (and in particular the flavor misalignment parametrized by W) is only seen in the U_1 interactions, while the Z' and G' couplings still respect (at tree-level) the $\mathrm{U}(2)_q$ and $\mathrm{U}(1)_{\ell_1} \times \mathrm{U}(1)_{\chi_1} \times \mathrm{U}(1)_{\ell_2+\chi_2}$ symmetries separately. This is analogous to the SM case with the CKM matrix and corresponds to the "Cabbibo mechanism" described in [34]. However, in contrast to the setup in [34], in our case this mechanism does not let us induce non-diagonal U_1 couplings among second- and third-generation SM fermions, but only among the light-families. For simplicity in the discussion, and in order to avoid large NP contributions to $\Delta F = 2$ observables and LFV transitions involving electrons, we set $W = \mathbb{1}$ and $\delta\lambda_q = \delta\lambda_\ell = 0$, enhancing the surviving flavor

JHEP07(2019)168

symmetry to $\mathrm{U}(1)_{\ell_1} \times \mathrm{U}(1)_{q_1+\chi_1}$. As a result, after SSB we obtain the following U_1 couplings in the fermion mass-eigenbasis

$$\beta'_L \xrightarrow{\langle \Omega_{1,3} \rangle} \beta_L = \mathcal{R}_{14}(\theta_{q_1})\, \mathcal{R}_{25}(\theta_{q_2})\, \mathrm{diag}(0,0,1,1,1)\, \mathcal{R}^\dagger_{25}(\theta_{\ell_2})$$
$$= \left(\begin{array}{ccc:cc} 0 & 0 & 0 & -s_{q_1} & 0 \\ 0 & s_{\ell_2} s_{q_2} & 0 & 0 & -c_{\ell_2} s_{q_2} \\ 0 & 0 & 1 & 0 & 0 \\ \hdashline 0 & 0 & 0 & c_{q_1} & 0 \\ 0 & -s_{\ell_2} c_{q_2} & 0 & 0 & c_{\ell_2} c_{q_2} \end{array}\right), \tag{3.9}$$

where $\mathcal{R}_{ij}(\theta)$ denotes a rotation of angle θ between the fermions i and j, and s_{q_i,ℓ_2} and c_{q_i,ℓ_2} are short for $\sin\theta_{q_i,\ell_2}$ and $\cos\theta_{q_i,\ell_2}$. The dashed lines in the matrix separate the 3×3 subsector of the chiral (SM) fermions from the vector-like ones. The mixing angles are defined in terms of Lagrangian parameters as

$$\tan\theta_{q_1} = \tan\theta_{q_2} = \frac{\lambda_q\, \omega_3}{\sqrt{2} M_\chi}\,, \quad \tan\theta_{\ell_2} = \frac{\lambda_\ell\, \omega_1}{\sqrt{2} M_\chi}\,. \tag{3.10}$$

The coupling structure in (3.9) coincides with the one obtained in [31, 32, 37] before EWSB. As argued in section 2.3, this coupling structure is not enough to provide a good fit to data since a sizable β_L^{23} coupling is required. The 2-3 misalignment can be achieved with the Yukawa interactions involving Ω_{15}. We have

$$-\mathcal{L} \supset \hat{\lambda}_{15}\, \bar{\psi}'_L \Omega_{15} \chi_R + \hat{\lambda}'_{15}\, \bar{\chi}_L \Omega_{15} \chi_R + \text{h.c.}\,, \tag{3.11}$$

where $\hat{\lambda}'_{15}$ is a 2×2 matrix and $\hat{\lambda}_{15}$ a 2-dimensional vector that we assume to be aligned with the second family, namely $\hat{\lambda}_{15}^\intercal = (0\ \lambda_{15})$.[6] As we did with the vector-like mass, we further assume $\hat{\lambda}'_{15}$ to be flavor universal, i.e. we fix $\hat{\lambda}'_{15} = \lambda'_{15}\, \mathbb{1}_{2\times 2}$. After SSB, the Lagrangian term proportional to $\hat{\lambda}'_{15}$ generates a mass splitting between vector-like quarks and leptons,

$$M_Q = M_\chi + \frac{1}{2\sqrt{6}}\, \lambda'_{15}\, \omega_{15}\,, \quad M_L = M_\chi - \frac{3}{2\sqrt{6}}\, \lambda'_{15}\, \omega_{15}\,. \tag{3.12}$$

On the other hand, the parameter λ_{15} acts as a new source of flavor breaking. After Ω_{15} takes a vev, it triggers the following explicit flavor symmetry breaking

$$\mathrm{U}(2)_\chi \xrightarrow{\lambda_{15}} \mathrm{U}(1)_{\chi_1}\,. \tag{3.13}$$

Analogously to the case discussed above, after SSB the term proportional to λ_{15} yields a mass-mixing between the third-generation and one of the vector-like fermions. However, since T_4^{15} commutes with the generators associated to the Z' and G', this breaking is only seen by the U_1 interactions, up to very small corrections. This way we are able to generate large non-diagonal U_1 interactions between ψ_L^3 and χ^2, proportional to λ_{15}, while in first

[6] Other orientations of $\hat{\lambda}_{15}$ can be reabsorbed into a redefinition of $\chi_{L,R}$ and do not affect the interactions discussed here.

JHEP07(2019)168

approximation (i.e. to first order in the flavor-breaking terms) the Z' and G' interactions remain unaffected, see appendix B. In combination with the mixing induced by the $\lambda_{q,\ell}$ terms, this translates into sizable contributions to $\beta_L^{23,32}$, while keeping flavor-changing neutral currents under control. More precisely, after SSB we end up with the following U_1 interactions in the fermion mass basis

$$\beta'_L \xrightarrow{\langle\Omega_{1,3,15}\rangle} \beta_L \approx \mathcal{R}_{14}(\theta_{q_1})\,\mathcal{R}_{25}(\theta_{q_2})\,\mathcal{R}_{35}(\chi_q)\,\mathrm{diag}(0,0,1,1,1)\,\mathcal{R}_{35}^\dagger(\chi_\ell)\,\mathcal{R}_{25}^\dagger(\theta_{\ell_2})$$
$$= \left(\begin{array}{ccc:cc} 0 & 0 & 0 & -s_{q_1} & 0 \\ 0 & s_{\ell_2}s_{q_2}c_\chi & s_{q_2}s_\chi & 0 & -c_{\ell_2}s_{q_2}c_\chi \\ 0 & -s_{\ell_2}s_\chi & c_\chi & 0 & c_{\ell_2}s_\chi \\ \hdashline 0 & 0 & 0 & c_{q_1} & 0 \\ 0 & -s_{\ell_2}c_{q_2}c_\chi & -c_{q_2}s_\chi & 0 & c_{\ell_2}c_{q_2}c_\chi \end{array}\right), \tag{3.14}$$

where $\chi \equiv \chi_\ell - \chi_q$ and the new mixing angles are related to the Lagrangian parameters by

$$\tan\chi_q = \frac{1}{2\sqrt{6}}\frac{\lambda_{15}\,\omega_{15}}{M_Q}\,, \qquad \tan\chi_\ell = \frac{-3}{2\sqrt{6}}\frac{\lambda_{15}\,\omega_{15}}{M_L}\,. \tag{3.15}$$

Note that at this point the expressions for θ_{q_i,ℓ_i} are slightly modified compared to those in (3.10). The new expressions read

$$\tan\theta_{q_1} = \frac{\lambda_q\,\omega_3}{\sqrt{2}M_Q}\,, \qquad \tan\theta_{q_2} = \frac{\lambda_q\,\omega_3}{\sqrt{2}M_Q}\,c_{\chi_q}\,, \qquad \tan\theta_{\ell_2} = \frac{\lambda_\ell\,\omega_1}{\sqrt{2}M_L}\,c_{\chi_\ell}\,. \tag{3.16}$$

Finally, the resulting physical masses for the vector-like fermions are given by

$$\begin{aligned} M_{Q_1} &= \sqrt{M_Q^2 + \frac{|\lambda_q|^2\,\omega_3^2}{2}}\,, & M_{Q_2} &= \sqrt{M_Q^2 + \frac{|\lambda_q|^2\,\omega_3^2}{2} + \frac{|\lambda_{15}|^2\,\omega_{15}^2}{24}}\,, \\ M_{L_1} &= M_L\,, & M_{L_2} &= \sqrt{M_L^2 + \frac{|\lambda_\ell|^2\,\omega_1^2}{2} + \frac{3\,|\lambda_{15}|^2\,\omega_{15}^2}{8}}\,. \end{aligned} \tag{3.17}$$

After EWSB, a final rotation to bring the SM fermions to their mass-eigenbasis is needed. The Yukawa interactions involving the Higgsses introduce new sources of breaking of the flavor symmetry in (3.5), whose structure fits well with the minimal U(2) picture in [88]. A detailed discussion of these symmetry-breaking terms and their connection to the SM fermion masses and mixing angles can be found in [32] (see also [37]). In particular, the rotation matrices that bring the SM fermions from the flavor basis defined in (2.3) to the mass-eigenbasis, $L_{d,\ell}$ and $R_{u,d,e}$, can be found in the appendix A of [32]. In this reference, the different breaking of the flavor symmetry are parametrized in terms of new mixing angles whose phenomenological constraints are also discussed. Here, for simplicity, we take $s_b = s_e = \phi_\tau = 0$ and fix $\alpha_d = \pi$ in these rotation matrices.[7] Under these assumptions,

[7] As shown in [32], (small) deviations from these values are possible and might even be welcome in the case of s_b if we allow for the CP violating phase $\phi_b \approx \pi/2$.

JHEP07(2019)168

the U_1 interactions in the mass basis for SM fermions can finally be written as

$$\beta'_L \xrightarrow{\langle\Omega_{1,3,15}\rangle\,,\,\langle H_{1,15}\rangle} \beta_L$$

$$\approx \left(\begin{array}{ccc:c} 0 & -|V_{td}/V_{ts}|\, c_d\, s_{\ell_2} s_{q_2} c_\chi & -|V_{td}/V_{ts}|\, c_d\, s_{q_2} s_\chi & -c_d\, s_{q_1} \quad -|V_{td}/V_{ts}|\, c_d\, c_{\ell_2} s_{q_2} c_\chi \\ 0 & c_d\, s_{\ell_2} s_{q_2} c_\chi & c_d\, s_{q_2} s_\chi & -|V_{td}/V_{ts}|\, c_d\, s_{q_1} \quad -c_d\, c_{\ell_2} s_{q_2} c_\chi \\ 0 & -s_{\ell_2} s_\chi - s_\tau\, c_\chi & c_\chi & 0 \qquad\qquad c_{\ell_2} s_\chi \\ \hdashline 0 & 0 & 0 & c_{q_1} \qquad\qquad 0 \\ 0 & -c_{q_2}(s_{\ell_2} c_\chi - s_\tau\, s_\chi) & -c_{q_2} s_\chi & 0 \qquad\qquad c_{\ell_2} c_{q_2} c_\chi \end{array}\right),$$

$$\beta'_d \xrightarrow{\langle\Omega_{1,3,15}\rangle\,,\,\langle H_{1,15}\rangle} \beta_d \approx e^{i\phi_d} \begin{pmatrix} 0 & 0 & 0 \\ 0 & 0 & 0 \\ 0 & \frac{m_\mu}{m_\tau}\, s_\tau & 1 \end{pmatrix}, \tag{3.18}$$

where $c_d \approx 0.98$ and ϕ_d is an arbitrary phase that we fix to $\phi_d = \pi$ to maximize the NP contributions to $R(D^{(*)})$ (see (2.6) and (2.7)). We stress that the latter choice does need to be enforced and, in presence of a more precise measurement of $\Delta R_D/\Delta R_{D^*}$ and/or polarization observables in $b \to c\tau\nu$ transitions, the value of ϕ_d could also be extracted from the low-energy fit.

This flavor structure for the U_1 couplings nicely matches the one discussed in section 2 (with $\beta_R \equiv \beta_d$). The only difference between the two structures is given by the non-zero values for $\beta_L^{d\mu}$ and $\beta_R^{b\mu}$, which were set to zero in (2.4). These two couplings are extremely suppressed (or can be chosen to be very small), justifying a posteriori having neglected them in section 2. In particular one has $|\beta_L^{d\mu}| = |V_{td}/V_{ts}||\beta_L^{s\mu}| \lesssim 0.01$ (taking into account the fit result for $|\beta_L^{s\mu}|$).[8] The size of $\beta_R^{b\mu}$ is not precisely fixed, but the phenomenological condition $|\beta_R^{b\mu}/\beta_L^{b\mu}| \lesssim 0.02$ (see section 2.2) can be obtained by imposing $|s_\tau| \lesssim 0.05$.

At this point we can address more precisely the question of which are the ingredients necessary to generate a sufficiently large $\beta_L^{s\tau}$. For the purpose of illustration, working in the limit of small mixing angle (i.e. small flavor symmetry-breaking terms), we get

$$\beta_L^{s\tau} \approx (\chi_\ell - \chi_q)\theta_{q_2} = -\lambda_{15}\lambda_q \frac{\omega_3\, \omega_{15}}{\sqrt{3}\, M_L\, M_Q} \left[1 + \mathcal{O}(\lambda'_{15})\right]. \tag{3.19}$$

As expected, $\beta_L^{s\tau}$ is proportional to the two flavor breaking parameters λ_{15} and λ_q, whose collective presence leads to the effective breaking of the $\mathrm{U}(2)_q$ symmetry in the U_1 couplings. As we show in the next section, the maximal size of these breaking terms is constrained by $\Delta F = 2$ amplitudes.

3.3 Vector leptoquark loops in the UV-complete model

We are now ready to compute the relevant one-loop effects mediated by the vector leptoquark. An interesting property of the U_1 couplings obtained in (3.18), arising as a

[8] Such a value of $\beta_L^{d\mu}$ has no impact on the low-energy observables considered so far. It would have an impact in $b \to d\ell\ell$ transitions, if these were measured more precisely in the future: there we expect corrections relative to the SM of the same order as in $b \to s\ell\ell$, given the $\mathrm{U}(2)_q$ relation $|\beta_L^{d\mu}/\beta_L^{s\mu}| = |V_{td}/V_{ts}|$. Similar effects in short-distance $s \to d\ell\ell$ amplitudes (contributing e.g. to $K_L \to \mu\mu$) are obscured by long-distance contributions and are, in practice, not detectable.

JHEP07(2019)168

consequence of the unitarity of the fermion-mixing matrices, is that $(\beta_L^\dagger \beta_L)_{ij}$ and $(\beta_L \beta_L^\dagger)_{ij}$ are diagonal in the SM sub-block, i.e. for $i,j = 1,2,3$. This property, analogous to the GIM mechanism in the SM, ensures a "flavor protection" in the U_1 loops. Thanks to this protection, we find that U_1 contributions to purely leptonic processes such as $\tau \to 3\mu$ and $\tau \to \mu\nu\nu$, or to semileptonic processes like $B \to K^{(*)}\nu\nu$, do not have a relevant phenomenological impact (see also [34, 43, 63]) and hence we do not include them in our discussion. Instead, we focus here on $\Delta F = 2$ and dipole transitions, which are more severely constrained.

3.3.1 $\Delta F = 2$ transitions

We parametrize the U_1 contributions to $\Delta F = 2$ observables by the following effective Lagrangians

$$\mathcal{L}_{\Delta B=2} = C_{B_i} \left(\bar{b}_L \gamma_\mu d_L^i\right)^2 , \qquad \mathcal{L}_{\Delta S=2} = C_K \left(\bar{s}_L \gamma_\mu d_L\right)^2 , \qquad \mathcal{L}_{\Delta C=2} = C_D \left(\bar{c}_L \gamma_\mu u_L\right)^2 . \tag{3.20}$$

The SM contribution to the $\Delta B = 2$ operator reads

$$C_{B_i}^{\rm SM}(m_b) \approx \frac{G_F^2 M_W^2}{4\pi^2} \left(V_{tb}^* V_{ti}\right)^2 S_0(x_t)\, \eta_B , \tag{3.21}$$

with η_B being a running factor, $S_0(x)$ the Inami-Lim function [89] and $x_t = m_t^2/M_W^2$. NP contributions to this operator mediated by the U_1 at one loop have been computed in [34]. The same result applies also to our model, given that the U_1 right-handed couplings in (3.18) do not contribute to this observable. We have

$$C_{B_i}^{U}(m_b) = -\frac{C_U^2 M_U^2\, G_F^2}{4\pi^2}\, \eta_U \sum_{\ell,\ell'} \lambda_{B_i}^{\ell} \lambda_{B_i}^{\ell'}\, F(x_\ell, x_{\ell'}) , \tag{3.22}$$

where η_U accounts for the running from M_U to m_b, $\lambda_{B_i}^{\ell} = \beta_L^{b\ell} \left(\beta_L^{i\ell}\right)^*$, $x_\ell = M_\ell^2/M_U^2$ (with M_ℓ the mass of the lepton running in the loop) and the loop function $F(x_\ell, x_{\ell'})$ can be found in [34]. In the evaluation of (3.22) we have removed x_ℓ-independent terms, which cancel after using the unitarity of the fermion-mixing matrices. The final result is finite only after all the fermions entering in the loop, including the vector-like leptons, are included. The dominant NP contribution is given by the most massive particle in the loop, in this case one of the vector-like leptons. Neglecting the SM lepton masses, we find

$$C_{B_i}(m_b) \equiv 1 + \frac{C_{B_i}^{U}(m_b)}{C_{B_i}^{\rm SM}(m_b)} \approx 1 + \frac{C_U^2 M_U^2}{M_W^2} \left(\frac{\beta_L^{bL_2} \beta_L^{iL_2\,*}}{V_{tb}^* V_{ti}}\right)^2 \frac{S_0(x_{L_2})}{S_0(x_t)}\, \frac{\eta_U}{\eta_B} . \tag{3.23}$$

Note that, due to the flavor structure in (3.18), we have $C_{B_d}^U \approx 0$, while the U_1 contribution to B_s-mixing can be sizable. Taking $c_{\ell_2} \approx 1$, we can use the relation $\beta_L^{bL_2} \beta_L^{sL_2} \approx -\beta_L^{b\tau} \beta_L^{s\tau}/c_d$ to write the B_s-mixing contribution in terms of the parameters used in section 2. Taking the bounds on $C_{B_s}(m_b)$ from Δm_s provided by UTfit [77], we extract an upper limit on M_{L_2} of a few TeV, see figure 5.

JHEP07(2019)168

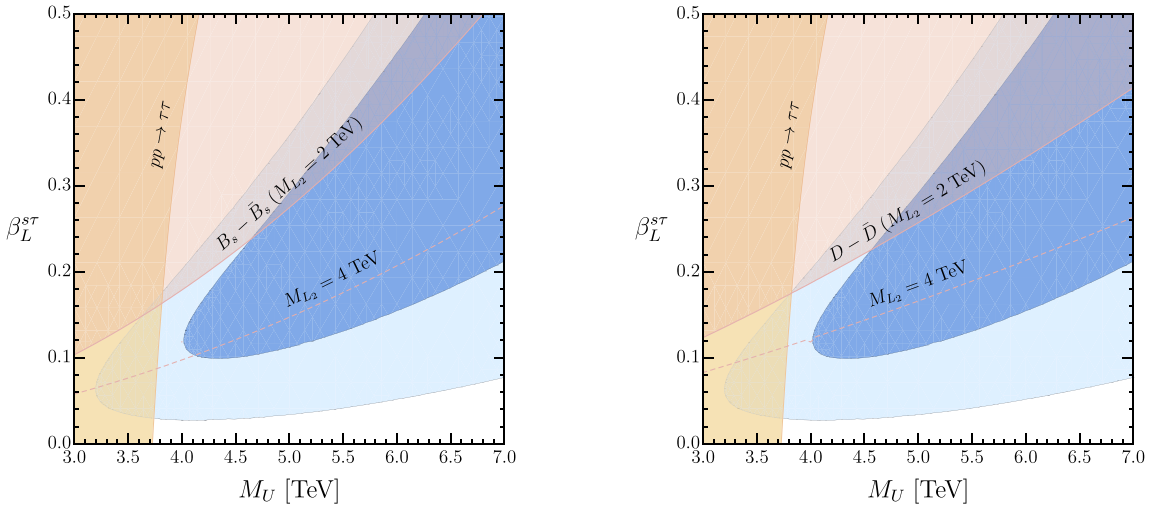

Figure 5. 95% CL constraints from $B_s - \bar{B}_s$ and $D - \bar{D}$ for different benchmarks values of the vector-like lepton mass M_{L_2} and with $g_U = 3.0$. The 1σ and 2σ regions preferred by the low-energy fit are shown in blue and light blue, respectively. For reference, we also show the high-p_T bound from $pp \to \tau\tau$ taken from [27] and discussed in section 2.4. In the right plot we fix $s_\chi = 0.55$ and $s_{\ell_2} = 0.15$.

It should be stressed that the growth of $\Delta F = 2$ amplitudes with the vector-like mass is an artifact due to our choice of expressing the result in terms of the β_L^{ij} couplings. Indeed working in the limit of small mixing, in analogy to eq. (3.19), C_{B_s} can be expressed as follows

$$C_{B_s}(m_b) \approx 1 + \frac{1}{24}\frac{\eta_U}{\eta_B}\frac{v^2}{M_Q^2}\left[\frac{g_U^4\omega_3^2\omega_{15}^2}{M_U^4}\right]\frac{\lambda_{15}^2\lambda_q^2}{y_t^2\,V_{ts}^2}\,(1+\rho)\,, \tag{3.24}$$

where y_t is the top-quark Yukawa coupling and ρ is an $\mathcal{O}(1)$ term depending on the details of the spectrum. This results exhibits the expected decoupling behavior with the NP masses and the power growth with the symmetry breaking parameters λ_{15} and λ_q. From eq. (3.24) it is evident that the B_s-mixing constrains the maximal size of λ_{15} and λ_q. On the other hand, if we wish to keep the couplings fixed (in particular $\beta_L^{s\tau}$) given the information derived from the low-energy fit, then the B_s-mixing bound can be translated into an upper bound on the vector-like masses (as shown in figure 5). From this point of view the situation resembles the SM case, where the charm quark was predicted in order to render the SM loop contribution finite [90], and a rough estimation of the charm mass was obtained from $K - \bar{K}$ mixing [91].

Proceeding in a similar way with $D - \bar{D}$ mixing we find[9]

$$C_D^U = -\frac{C_U^2 M_U^2\, G_F^2}{4\pi^2}\sum_{\ell,\ell'}\lambda_D^\ell\lambda_D^{\ell'}\,F(x_\ell, x_{\ell'})\,, \tag{3.25}$$

[9]Contrary to the $\Delta B = 2$ case, we have tree-level contributions to $\Delta C = 2$ transitions, meditated by the Z' and G'. In the U(2)$_q$-preserving limit, these contributions are proportional to $(V_{ub}^* V_{cb})^2$ and therefore negligibly small [34]. In our loop calculation, we consistently remove terms of $\mathcal{O}[(V_{ub}^* V_{cb})^2]$, which are negligible compared to their tree-level counterparts.

JHEP07(2019)168

where $\lambda_D^\ell = V_{ui}^* V_{cj} (\beta_L^{i\ell})^* \beta_L^{j\ell}$. We get important constraints from NP contributions to the imaginary part of C_D^U. We can interpret these constraints as a bound on $\beta_L^{s\tau}$ as a function of M_U, once we fix the vector-like lepton masses, s_χ and s_{ℓ_2}. This is shown in figure 5 where we use the latest UTfit analysis for the $D-\bar{D}$ constraint [92, 93]. On the other hand, as it happens with B_d-mixing, the contributions to $K-\bar{K}$ mixing are suppressed by the SM lepton masses and are thus negligible.

3.3.2 Dipole contributions

It was noted in [63] that a large $\beta_L^{s\tau}$ could yield sizable $b \to s$ dipole contributions mediated by the U_1 at one loop. Recasting the results in [94, 95] and neglecting terms proportional to m_s, we find ($\ell = \mu, \tau, L_2$)

$$\begin{aligned}\Delta\mathcal{C}_{7(8)} = \frac{C_U}{V_{tb}V_{ts}^*}\sum_\ell \beta_L^{s\ell}(\beta_L^{b\ell})^*\left(\frac{x_\ell\left(4+25x_\ell+x_\ell^2\right)}{24(1-x_\ell)^3}+\frac{x_\ell^2(3+2x_\ell)\log x_\ell}{4(1-x_\ell)^4}\right)\\ +\beta_L^{s\tau}(\beta_R^{b\tau})^*\frac{m_\tau}{m_b}\left(\frac{4+25x_\tau+x_\tau^2}{12(1-x_\tau)^2}+\frac{x_\tau(3+2x_\tau)\log x_\tau}{2(1-x_\tau)^3}\right),\end{aligned} \tag{3.26}$$

and $\Delta\mathcal{C}_{7',8'} \approx 0$ (see appendix A for the Wilson coefficient definitions). For $\beta_R^{b\tau} = -1$ we find that the LR term gives the dominant contribution. Using the low-energy fit values from section 2.3, and taking into account the running from the TeV scale to m_b [95], we get $\Delta\mathcal{C}_{7,8}(m_b) \sim \mathcal{O}(10^{-3})$, well below the current bounds [62]. We find that the LL contribution is smaller by two orders of magnitude compared to the one found in [63]. This difference is due to the cancellation of the x_ℓ-independent terms proportional to $\beta_L^{s\tau}(\beta_L^{b\tau})^*$, once we also include the vector-like lepton in the loop. Once more, we note the importance of computing these loops in a UV-complete model.

The dominant (chirally enhanced) contribution to $\tau \to \mu\gamma$ was already computed in the dynamical model in section 2. The full U_1 contribution, now calculable in the UV-complete model, is found to be [94] ($q = s, b, Q_1, Q_2$)

$$\begin{aligned}\mathcal{B}(\tau\to\mu\gamma) = \frac{1}{\Gamma_\tau}\frac{\alpha}{4096\pi^4}\frac{m_\tau^3 m_b^2}{v^4}C_U^2\Bigg|2\,\beta_L^{b\mu}(\beta_R^{b\tau})^*\left(\frac{4-23x_b+x_b^2}{(1-x_b)^2}-\frac{6x_b(1+2x_b)\log x_b}{(1-x_b)^3}\right)\\ -\frac{m_\tau}{m_b}\sum_q \beta_L^{q\mu}(\beta_L^{q\tau})^*\left(\frac{3x_q^2(5+x_q)}{(1-x_q)^3}+\frac{6x_q^2(1+2x_q)\log x_q}{(1-x_q)^4}\right)\Bigg|^2,\end{aligned} \tag{3.27}$$

where we have ignored terms proportional to m_μ and, as in the previous computations, we have used the unitarity of the fermion-mixing matrices to remove the x_q-independent terms in the LL contribution. We have explicitly checked that when $\beta_R^{b\tau} = -1$ the LL contributions are much smaller than the ones included in (2.15), which justifies having neglected them in the low-energy fit.

3.4 Constraints on the new fields

The UV-complete model introduced in section 3.1 contains additional fields beyond the U_1 that could potentially alter some of the results obtained in section 2. In what follows, we discuss the main constraints on these particles

JHEP07(2019)168

- **Additional vectors.** If we assume perfect alignment to down-type quarks, as we did in (3.18), the Z' and G' couplings to fermions are given in appendix B. In this limit, the only $\Delta F = 2$ amplitude receiving relevant tree-level contributions from Z' and G' exchange is $D - \bar{D}$ mixing.[10] Using the same notation as in (3.20) for the Wilson coefficient and taking the mixing angles in (3.16), we can write the contribution to $\Delta C = 2$ transitions as (see also [32, 34])

$$C_1^D\big|_{\text{tree}} \approx \frac{4G_F}{\sqrt{2}}\left(C_{Z'} + \frac{C_{G'}}{3}\right)(V_{ub}^* V_{cb})^2 \left(1 - s_{q_1}^2 - c_d^2\, s_{q_1}^2\, s_{\chi_q}^2 \left|\frac{V_{tb}}{V_{ts}}\right|^2\right)^2 , \tag{3.28}$$

where $C_{Z'}$ and $C_{G'}$ are given by

$$C_{Z'} = \frac{g_Y^2}{24\, g_1^2}\,\frac{g_4^2 v^2}{4\, M_{Z'}^2}\,, \quad C_{G'} = \frac{g_c^2}{g_3^2}\,\frac{g_4^2 v^2}{4\, M_{G'}^2}\,. \tag{3.29}$$

In the $\mathrm{U}(2)_q$-preserving limit, i.e. when $s_{q_1} s_{\chi_q} = 0$, these contributions are strongly CKM-suppressed and the net effect on C_1^D is of $\mathcal{O}(10^{-9})$ TeV^{-2} for both real and imaginary parts, well compatible with the current limits from UTFit [92, 93]. On the other hand $\mathrm{U}(2)_q$-breaking effects, parametrized by $s_{q_1} s_{\chi_q}$, are CKM-enhanced compared with the latter contribution and could be potentially dangerous. Using typical values for the model parameters, we estimate that the $\mathrm{U}(2)_q$-breaking term can be as large as $|s_{q_1} s_{\chi_q}| \approx 0.07$, while remaining consistent with the $D - \bar{D}$ constraint. Using the relations in (3.15), we find that it is possible to obtain sizable values for $\beta_L^{s\tau}$, as required by the low-energy fit, while keeping the NP contributions to $D - \bar{D}$ well below the current bounds.

The additional vectors are in the interesting range for high-p_T searches at LHC. The related collider signatures have been extensively analyzed in general terms in [27]. Here we comment on the main implications for the benchmark $g_4 = 3.0$ (implying $g_4 \gg g_3 \gg g_1$), for which the Z' and G' interactions to light-generation quarks and leptons are suppressed. The most important constraint on the G' is obtained from $pp \to tt$, which sets a lower limit on its mass of $M_{G'} \gtrsim 3.5\,\text{TeV}$. Given the mass relation between the U_1 and G' (see (3.3) taking $g_4 \gg g_3$),

$$M_{G'} \approx M_U \sqrt{\frac{2\,\omega_3^2}{\omega_1^2 + \omega_3^2 + \frac{4}{3}\omega_{15}^2}}\,, \tag{3.30}$$

we find that current high-p_T bounds on the G' are typically less constraining (although comparable) than the ones on the U_1 for most of the parameter space. This is in contrast to other UV completions where the vector leptoquark only couples to left-handed fermions, as e.g. in [34]. The most relevant channel for direct searches on the Z' is $pp \to \tau\tau$, from which we obtain a mass limit of $M_{Z'} \gtrsim 2.5$. The Z' contributions to this channel could potentially affect the discussion in section 2.4. However, these contributions drop fast with increasing Z' mass and become negligible once $M_{Z'} \gtrsim 3.0\,\text{TeV}$.

[10] A small tree-level effect is also generated in the $K - \bar{K}$ mixing amplitude. Given its smallness and the fact that it mostly contributes to the real part of the mixing amplitude, this effect is unobservable.

JHEP07(2019)168

- **Vector-like fermions.** Vector-like fermions are predicted to be among the lightest new states in the model. High-p_T searches involving these particles therefore constitute a very interesting probe for the proposed scenario. Most of the results obtained in [34] apply also to our model. However, in our case the vector resonances and vector-like fermions are heavier, resulting in typically smaller production cross sections. As shown in section 3.3.1, vector-like lepton masses are expected to lie around 2–4 TeV. A mass splitting between vector-like quarks and leptons is generated after Ω_{15} takes a vev (see (3.12)), resulting in vector-like quarks masses that are around one TeV larger than the ones of the vector-like leptons.

  As in [34], the dominant production mechanism for the vector-like quarks is not via QCD interactions but via the G' through the processes $q\bar{q} \to G' \to Q\bar{Q}, Q\bar{q}, q\bar{Q}$. The G' dominantly decays to vector-like pairs while the SM-vector-like combination is suppressed by one power of $s_{q_{1,2}}$. Vector-like leptons are produced via electroweak interactions. Neutral current processes receive additional contributions from Z'-assisted production which is stronger than the eletroweak production by more than one order of magnitude. Analogously to the vector-like quark case, mixed Z' decays involving a SM and a vector-like lepton are suppressed by one power of s_{ℓ_2}. We implement the model in `FeynRules` [96] and use `Madgraph5_aMC@NLO` [97] to compute the production cross-sections. We find that the production cross-sections for both vector-like quarks and leptons are well below 1 fb in the relevant range of model parameters, and therefore out of the LHC reach.

  Second-family vector-like fermions can have sizable couplings to the Higgs, and they are expected to decay dominantly to a third-generation SM fermion of the same type and a h, W or Z. Current limits on pair-produced vector-like quarks and leptons with these decay channels are of $\mathcal{O}(10)$ fb [98, 99]. The situation is different for the first-family vector-like fermions. As in [34], their coupling to the Higgs are extremely suppressed by the first-generation fermion masses, so they are expected to decay predominantly to three third-generation SM fermions via an off-shell heavy vector.[11] In this case, the vector-like signatures in the detector contain multiple jets and leptons and are rich with b-tags and τ-tags. While a dedicated analysis on these signatures is needed, one can extract a rough estimate on the production cross-section by comparing with existing supersymmetry searches [100]. The limit found in [34] is around $5 - 15$ fb, depending on the decay topologies.

- **Additional scalars.** A dedicated analysis of the scalar sector of the model is beyond the scope of this paper (a detailed analysis for a very similar setup can be found in [34]). The masses of the additional scalars depend on the scalar potential parameters, which are mostly unconstrained, but they are expected to be around a few TeV. The Yukawa couplings of the radial excitations in $\Omega_{1,3,15}$ necessarily involve a SM and a vector-like fermion, see (3.6) and (3.11). Therefore, they can only affect

[11] This decay channel can also dominate over the two-body decay for the second-generation vector-like fermions whose couplings to the Higgs are accidentally suppressed. This is for instance the case for the down-type vector-like quark if we assume perfect alignment to SM down-type quarks, as we did in (3.18).

JHEP07(2019)168

low-energy observables at the one-loop level. Moreover, flavor-changing transitions are protected by the same flavor structure that controls the vector boson interactions. As a result, we conclude that these scalars do not yield relevant effects at low energies. Apart from the additional Higgs doublet, the H_{15} also features a R_2 and a $\tilde{R}_2$ leptoquarks and a color octet charged under $\mathrm{SU}(2)_L$. These scalars have Yukawa interactions with two SM fermions and could potentially mediate relevant low-energy effects. Also in this case, the Yukawa interactions present the same flavor structure discussed in 3.2: dominant couplings to third-generation fermions, with small couplings to left-handed light-generation fermions and negligible couplings to right-handed light-generation fermions. The R_2 leptoquark was recently proposed as a solution to the $R_{D^{(*)}}$ anomalies [36]. However in our model the R_2 contributions to these observables are negligible due to the smallness of the light-generation right-handed couplings. On the other hand, the R_2 leptoquark could yield potentially large contributions to $\mathcal{B}(\tau \to \mu\gamma)$ at the one-loop level which are chiral enhanced by a factor m_t/m_τ, see e.g. [101]. We find that the R_2 contributions to this observable are below the current bounds provided its Yukawa interactions are of $\mathcal{O}(10^{-1})$, for a mass of 2 TeV. The $\tilde{R}_2$ leptoquark has also been proposed as a possible explanation of the $R_{D^{(*)}}$ anomalies if one introduces a light ν_R that fakes the SM ones, as e.g. in [52, 102]. We will not consider this possibility here.

Concerning direct searches, the most interesting states to look for at high-p_T are the colored ones, since they can be produced via QCD interactions. Following the discussion in [34] (see also [103]), we conclude that the production cross-sections of the radial modes in $\Omega_{1,3,15}$ are small enough to avoid detection at the LHC provided their masses are around a few TeV. Similar conclusions also hold for the charged color-octect and the R_2 and $\tilde{R}_2$ leptoquarks [35, 45, 104].

We therefore conclude that the presence of the additional particles does not affect the phenomenological implications of the U_1 derived in terms of the simplified model. However, the UV-complete model presents many interesting signatures that go beyond the simplified setup and whose exploration could be an essential ingredient to test the U_1 solution of the B-anomalies and possibly reconstruct the underlying NP model.

For the sake of completeness, we report here a benchmark point that provides a good low-energy fit and satisfies the high-p_T constraints discussed in section 2, as well as the additional low-energy constrains discussed above:

$$\begin{aligned} &g_4 = 3.0\,, \quad \omega_1 = 1.0\ \text{TeV}\,, \quad \omega_3 = 2.2\ \text{TeV}\,, \quad \omega_{15} = 1.5\ \text{TeV}\,, \quad M_\chi = 3.0\ \text{TeV}\,, \\ &\lambda_\ell = 0.25\,, \quad \lambda_q = 0.25\,, \qquad \lambda_{15} = -1.2\,, \qquad \lambda'_{15} = 1.0\,, \qquad s_\tau = 0.05\,. \end{aligned} \tag{3.31}$$

From these values we obtain the following spectrum

$$\begin{aligned} M_U = 4.5\ \text{TeV}\,, \qquad M_{Z'} = 3.5\ \text{TeV}\,, \qquad M_{G'} = 5.0\ \text{TeV}\,, \\ M_{Q_1} \approx M_{Q_2} = 3.3\ \text{TeV}\,, \qquad M_{L_1} = 2.1\ \text{TeV}\,, \qquad M_{L_2} = 2.3\ \text{TeV}\,, \end{aligned} \tag{3.32}$$

and mixing angles $\{s_{\ell_2}, s_{q_1}, s_\chi, s_{\chi_q}, s_{\chi_\ell}\} = \{0.12, 0.21, 0.55, -0.11, 0.46\}$, resulting in the following effective leptoquark couplings: $\{\beta_R^{b\tau}, \beta_L^{b\tau}, \beta_L^{s\tau}, \beta_L^{b\mu}, \beta_L^{s\mu}, \beta_L^{d\tau}\} =$

JHEP07(2019)168

$\{-1.0, 0.84, 0.11, -0.11, 0.02, -0.02\}$. This benchmark point should not be considered as a particularly favored configuration. It is only an illustration that is possible to reach the allowed region of the spectrum consistent with data (figures 4 and 5), as well as the U_1 couplings identified by the low-energy fit (figure 2), with very reasonable Lagrangian parameters. We stress in particular the smallness of the Yukawa couplings in (3.31), which do not raise perturbativity issues up to very high energy scales. The only tuning of the model is the ansatz in (3.7) for the $\mathrm{U}(2)_q \times \mathrm{U}(2)_\ell$ flavor symmetry breaking terms, and their alignment to the down-type quark and charged-lepton mass-eigenstate basis (signaled by the smallness of s_b and s_τ). However, these are radiatively stable conditions that can be enforced via suitable dynamical constraints on the symmetry-breaking fields.

4 Conclusions

Among the different options proposed to explain the hints of LFU violation observed in B-meson decays, the hypothesis of a $\mathrm{SU}(2)_L$-singlet vector leptoquark (U_1) stands for its simplicity and effectiveness. In this paper we have presented a thorough investigation of this hypothesis from a twofold perspective: first using a simplified-model/EFT approach, taking into account recent results from B-physics observables and high-p_T searches, and then presenting a more complete model with a consistent UV behavior.

Employing the simplified model we have shown that a right-handed coupling for the U_1, mainly aligned to the third-generation, can be a virtue rather than a problem. This coupling, neglected in most previous studies, can yield a very good fit of the $b \to c$ anomalies without significant drawbacks. The outcome of the low-energy fit with the inclusion of right-handed couplings has been presented in section 2.3. A key difference with respect to previous studies is the strong enhancement (compared to the SM predictions) of the rates for helicity-suppressed modes with tau leptons, in particular $B_s \to \tau^+\tau^-$ and $B_s \to \tau\mu$. The experimental search of these decays modes, whose expectation is not far from present bounds, could provide a smoking-gun signature for this framework (or could lead us to rule it out). An additional important implication of the right-handed coupling for the U_1 is the larger impact on $b \to c$ anomalies at fixed U_1 mass. This fact, together with the reduced deviation from the SM indicated by the recent Belle analysis [5], leads to an excellent compatibility between low- and high-energy data in this framework, at least at present. Interestingly enough, the preferred mass-coupling range for the U_1 inferred by the anomalies is well within the reach of direct searches at the HL-LHC (see figure 4).

In the second part of the paper we have shown how a simple extension of the matter content of the model proposed in [31], based on a flavor deconstruction of the original Pati-Salam gauge group, provides a good UV completion for the U_1 with the precise couplings to SM fermions required to describe current data. The field content of the model is summarized in table 2. The most important consequence following from the requirement of a consistent UV completion is the necessity of extra TeV scale fields, with interesting high-p_T signatures that cannot be deduced within the simplified model. These new states include both a color-octet (G') and a color singlet (Z') vector field, as extensively discussed in [28, 31, 32, 37], and a pair of vector-like quarks and leptons. As we have shown, and as

JHEP07(2019)168

already pointed out in [34], the $\Delta F = 2$ constraints imply that the vector-like leptons are likely to be the lightest exotic states.

In conclusion, our analysis reinforces the phenomenological success of the vector leptoquark hypothesis in explaining the hints of LFU violation observed in B-meson decays, taking into account all available low- and high-energy data. We also confirm the compatibility of this hypothesis with motivated extensions of the SM based on the idea of flavor non-universal gauge interactions [31], which could provide an explanation for the long-standing puzzle of quark and lepton masses.

Acknowledgments

We thank Riccardo Barbieri for interesting discussions and we are grateful to Joaquim Matias and Javier Virto for providing us their results for the fit to $b \to s\ell\ell$ data prior to publication. This research was supported in part by the Swiss National Science Foundation (SNF) under contract 200021-159720.

A The weak effective Hamiltonian

Semileptonic and dipole $b \to s$ transitions are commonly parameterized in terms of the so-called Weak Effective Theory (WET) [105–107]

$$\mathcal{H}_{\rm WET} \supset -\frac{4G_F}{\sqrt{2}}\,\frac{e^2}{16\pi^2}\,V_{tb}V_{ts}^*\sum_i \Big[\mathcal{C}_i\,\mathcal{O}_i + h.c.\Big]\,, \tag{A.1}$$

where the operators

$$\begin{aligned}
\mathcal{O}_9^\ell &= (\bar{s}\gamma_\mu P_L b)\,\big(\bar{\ell}\gamma^\mu \ell\big)\,, & \mathcal{O}_{9'}^\ell &= (\bar{s}\gamma_\mu P_R b)\,\big(\bar{\ell}\gamma^\mu \ell\big)\,,\\
\mathcal{O}_{10}^\ell &= (\bar{s}\gamma_\mu P_L b)\,\big(\bar{\ell}\gamma^\mu\gamma_5 \ell\big)\,, & \mathcal{O}_{10'}^\ell &= (\bar{s}\gamma_\mu P_R b)\,\big(\bar{\ell}\gamma^\mu\gamma_5 \ell\big)\,,\\
\mathcal{O}_S^\ell &= m_b(\bar{s}P_R b)(\bar{\ell}\ell)\,, & \mathcal{O}_{S'}^\ell &= m_b(\bar{s}P_L b)(\bar{\ell}\ell)\,,\\
\mathcal{O}_P^\ell &= m_b(\bar{s}P_R b)(\bar{\ell}\gamma_5\ell)\,, & \mathcal{O}_{P'}^\ell &= m_b(\bar{s}P_L b)(\bar{\ell}\gamma_5\ell)\,,\\
\mathcal{O}_7 &= \frac{m_b}{e}\,(\bar{s}\,\sigma_{\mu\nu}\,P_R\,b)\;F^{\mu\nu}, & \mathcal{O}_{7'} &= \frac{m_b}{e}\,(\bar{s}\,\sigma_{\mu\nu}\,P_L\,b)\;F^{\mu\nu},\\
\mathcal{O}_8 &= \frac{g_c\,m_b}{e^2}\,(\bar{s}\,\sigma_{\mu\nu}\,P_R\,T^a\,b)\;G^{\mu\nu\,a}, & \mathcal{O}_{8'} &= \frac{g_c\,m_b}{e^2}\,(\bar{s}\,\sigma_{\mu\nu}\,P_L\,T^a\,b)\;G^{\mu\nu\,a}\,,
\end{aligned} \tag{A.2}$$

with $\ell = e, \mu, \tau$ and $P_{L,R} = 1/2(1 \mp \gamma_5)$. The corresponding Wilson coefficients are parametrized as $\mathcal{C}_i^\ell = \mathcal{C}_i^{\rm SM} + \Delta\mathcal{C}_i^\ell$, where $\mathcal{C}_i^{\rm SM}$ denotes the SM contribution and $\Delta\mathcal{C}_i^\ell$ encodes possible NP effects.

B Z' and G' couplings to fermions

For completeness, in this section we provide the Z' and G' couplings to fermions in their mass eigenbasis. Collecting the left-handed fermions in 5-dimensional multiplets,

JHEP07(2019)168

as in (3.4), we obtain

$$\mathcal{L}_{G'} \supset g_c \frac{g_4}{g_3} G'^a_\mu \left[\kappa_q (\bar\Psi_q \gamma^\mu T^a \Psi_q) + \kappa_u (\bar u_R \gamma_\mu T^a u_R) + \kappa_d (\bar d_R \gamma_\mu T^a d_R) + \kappa_Q (\bar Q_R \gamma_\mu T^a Q_R)\right],$$
$$\mathcal{L}_{Z'} \supset \frac{g_Y}{2\sqrt{6}} \frac{g_4}{g_1} Z'_\mu \left[\xi_q (\bar\Psi_q \gamma^\mu \Psi_q) + \xi_u (\bar u_R \gamma^\mu u_R) + \xi_d (\bar d_R \gamma^\mu d_R) + \xi_Q (\bar Q_R \gamma_\mu Q_R) - 3\xi_\ell (\bar\Psi_\ell \gamma^\mu \Psi_\ell)\right.$$
$$\left. - 3\xi_e (\bar e_R \gamma^\mu e_R) - 3\xi_L (\bar L_R \gamma_\mu L_R)\right]. \tag{B.1}$$

Using the same flavor assumptions as in section 3.2, the coupling matrices are given by

$$\kappa_q \approx \left(\begin{array}{ccc:cc} c_d^2(s_{q_1}^2 - c_{q_1}^2 g_3^2/g_4^2) & c_d^2 |V_{td}/V_{ts}| (s_{q_1}^2 - s_{q_2}^2) & 0 & -c_d c_{q_1} s_{q_1} & |V_{td}/V_{ts}| c_d c_{q_2} s_{q_2} \\ c_d^2 |V_{td}/V_{ts}| (s_{q_1}^2 - s_{q_2}^2) & c_d^2 (s_{q_2}^2 - c_{q_2}^2 g_3^2/g_4^2) & 0 & -|V_{td}/V_{ts}| c_d c_{q_1} s_{q_1} & -c_d c_{q_2} s_{q_2} \\ 0 & 0 & 1 & 0 & 0 \\ \hdashline -c_d c_{q_1} s_{q_1} & -|V_{td}/V_{ts}| c_d c_{q_1} s_{q_1} & 0 & c_{q_1}^2 & 0 \\ |V_{td}/V_{ts}| c_d c_{q_2} s_{q_2} & -c_d c_{q_2} s_{q_2} & 0 & 0 & c_{q_2}^2 \end{array}\right), \tag{B.2}$$

$$\xi_q \approx \left(\begin{array}{ccc:cc} c_d^2 s_{q_1}^2 & c_d^2 |V_{td}/V_{ts}| (s_{q_1}^2 - s_{q_2}^2) & 0 & -c_d c_{q_1} s_{q_1} & |V_{td}/V_{ts}| c_d c_{q_2} s_{q_2} \\ c_d^2 |V_{td}/V_{ts}| (s_{q_1}^2 - s_{q_2}^2) & c_d^2 s_{q_2}^2 & 0 & -|V_{td}/V_{ts}| c_d c_{q_1} s_{q_1} & -c_d c_{q_2} s_{q_2} \\ 0 & 0 & 1 & 0 & 0 \\ \hdashline -c_d c_{q_1} s_{q_1} & -|V_{td}/V_{ts}| c_d c_{q_1} s_{q_1} & 0 & c_{q_1}^2 & 0 \\ |V_{td}/V_{ts}| c_d c_{q_2} s_{q_2} & -c_d c_{q_2} s_{q_2} & 0 & 0 & c_{q_2}^2 \end{array}\right), \tag{B.3}$$

$$\xi_\ell \approx \left(\begin{array}{ccc:cc} 0 & 0 & 0 & 0 & 0 \\ 0 & s_{\ell_2}^2 & -s_\tau & 0 & -c_{\ell_2} s_{\ell_2} \\ 0 & -s_\tau & 1 & 0 & -s_\tau c_{\ell_2} s_{\ell_2} \\ \hdashline 0 & 0 & 0 & 1 & 0 \\ 0 & -c_{\ell_2} s_{\ell_2} & -s_\tau c_{\ell_2} s_{\ell_2} & 0 & c_{\ell_2}^2 \end{array}\right), \tag{B.4}$$

$$\kappa_u \approx \kappa_d \approx \xi_u \approx \xi_d \approx \xi_e \approx \mathbb{1}_{3\times 3}, \qquad \kappa_Q \approx \xi_Q \approx \xi_L \approx \mathbb{1}_{2\times 2}, \tag{B.5}$$

where we neglected terms of $\mathcal{O}(g_1^2/g_4^2)$ and $\mathcal{O}(s_{q_{1,2}} g_3^2/g_4^2)$. Note that the small breaking of $\mathrm{U}(2)_q$ mentioned in section 3.2 has to do with the fact that $s_{q_1} \neq s_{q_2}$. From (3.16), we can see that the difference between the two angles is sub-leading and therefore small enough to pass the stringent constraints from $D - \bar D$ mixing, see section 3.4. We remind the reader that these interactions are given in the flavor basis for the $\mathrm{SU}(2)_L$-doublets defined in (2.3).

References

[1] BaBar collaboration, *Measurement of an excess of $\bar B \to D^{(*)} \tau^- \bar\nu_\tau$ decays and implications for charged Higgs bosons*, *Phys. Rev.* **D 88** (2013) 072012 [arXiv:1303.0571] [INSPIRE].

JHEP07(2019)168

[2] LHCb collaboration, *Measurement of the ratio of branching fractions* $\mathcal{B}(\bar{B}^0 \to D^{*+}\tau^-\bar{\nu}_\tau)/\mathcal{B}(\bar{B}^0 \to D^{*+}\mu^-\bar{\nu}_\mu)$, *Phys. Rev. Lett.* **115** (2015) 111803 [*Erratum ibid.* **115** (2015) 159901] [arXiv:1506.08614] [INSPIRE].

[3] BELLE collaboration, *Measurement of the τ lepton polarization and $R(D^*)$ in the decay $\bar{B} \to D^*\tau^-\bar{\nu}_\tau$*, *Phys. Rev. Lett.* **118** (2017) 211801 [arXiv:1612.00529] [INSPIRE].

[4] LHCb collaboration, *Test of lepton flavor universality by the measurement of the $B^0 \to D^{*-}\tau^+\nu_\tau$ branching fraction using three-prong τ decays*, *Phys. Rev.* **D 97** (2018) 072013 [arXiv:1711.02505] [INSPIRE].

[5] BELLE collaboration, *Measurement of $R(D)$ and $R(D^*)$ with a semileptonic tag at Belle*, Moriond EW 2019, (2019).

[6] LHCb collaboration, *Test of lepton universality using $B^+ \to K^+\ell^+\ell^-$ decays*, *Phys. Rev. Lett.* **113** (2014) 151601 [arXiv:1406.6482] [INSPIRE].

[7] LHCb collaboration, *Test of lepton universality with $B^0 \to K^{*0}\ell^+\ell^-$ decays*, *JHEP* **08** (2017) 055 [arXiv:1705.05802] [INSPIRE].

[8] LHCb collaboration, *Search for lepton-universality violation in $B^+ \to K^+\ell^+\ell^-$ decays*, CERN-EP-2019-043, CERN, Geneva, Switzerland (2019).

[9] BELLE collaboration, *Study of lepton universality at Belle*, Moriond EW 2019, (2019).

[10] B. Bhattacharya, A. Datta, D. London and S. Shivashankara, *Simultaneous explanation of the R_K and $R(D^{(*)})$ puzzles*, *Phys. Lett.* **B 742** (2015) 370 [arXiv:1412.7164] [INSPIRE].

[11] R. Alonso, B. Grinstein and J. Martin Camalich, *Lepton universality violation and lepton flavor conservation in B-meson decays*, *JHEP* **10** (2015) 184 [arXiv:1505.05164] [INSPIRE].

[12] A. Greljo, G. Isidori and D. Marzocca, *On the breaking of lepton flavor universality in B decays*, *JHEP* **07** (2015) 142 [arXiv:1506.01705] [INSPIRE].

[13] L. Calibbi, A. Crivellin and T. Ota, *Effective field theory approach to $b \to s\ell(\ell')$, $B \to K(*)\nu\bar{\nu}$ and $B \to D(*)\tau\nu$ with third generation couplings*, *Phys. Rev. Lett.* **115** (2015) 181801 [arXiv:1506.02661] [INSPIRE].

[14] R. Barbieri, G. Isidori, A. Pattori and F. Senia, *Anomalies in B-decays and U(2) flavour symmetry*, *Eur. Phys. J.* **C 76** (2016) 67 [arXiv:1512.01560] [INSPIRE].

[15] G. Hiller and M. Schmaltz, *R_K and future $b \to s\ell\ell$ physics beyond the Standard Model opportunities*, *Phys. Rev.* **D 90** (2014) 054014 [arXiv:1408.1627] [INSPIRE].

[16] D. Ghosh, M. Nardecchia and S.A. Renner, *Hint of lepton flavour non-universality in B meson decays*, *JHEP* **12** (2014) 131 [arXiv:1408.4097] [INSPIRE].

[17] I. de Medeiros Varzielas and G. Hiller, *Clues for flavor from rare lepton and quark decays*, *JHEP* **06** (2015) 072 [arXiv:1503.01084] [INSPIRE].

[18] S. Fajfer and N. Košnik, *Vector leptoquark resolution of R_K and $R_{D^{(*)}}$ puzzles*, *Phys. Lett.* **B 755** (2016) 270 [arXiv:1511.06024] [INSPIRE].

[19] I. Doršner, S. Fajfer, A. Greljo, J.F. Kamenik and N. Košnik, *Physics of leptoquarks in precision experiments and at particle colliders*, *Phys. Rept.* **641** (2016) 1 [arXiv:1603.04993] [INSPIRE].

[20] D.A. Faroughy, A. Greljo and J.F. Kamenik, *Confronting lepton flavor universality violation in B decays with high-p_T tau lepton searches at LHC*, *Phys. Lett.* **B 764** (2017) 126 [arXiv:1609.07138] [INSPIRE].

JHEP07(2019)168

[21] A. Greljo and D. Marzocca, *High-p_T dilepton tails and flavor physics*, *Eur. Phys. J.* **C 77** (2017) 548 [arXiv:1704.09015] [INSPIRE].

[22] B. Diaz, M. Schmaltz and Y.-M. Zhong, *The leptoquark hunter's guide: pair production*, *JHEP* **10** (2017) 097 [arXiv:1706.05033] [INSPIRE].

[23] G. Hiller, D. Loose and I. Nišandžić, *Flavorful leptoquarks at hadron colliders*, *Phys. Rev.* **D 97** (2018) 075004 [arXiv:1801.09399] [INSPIRE].

[24] S. Bansal, R.M. Capdevilla, A. Delgado, C. Kolda, A. Martin and N. Raj, *Hunting leptoquarks in monolepton searches*, *Phys. Rev.* **D 98** (2018) 015037 [arXiv:1806.02370] [INSPIRE].

[25] M. Schmaltz and Y.-M. Zhong, *The leptoquark hunter's guide: large coupling*, *JHEP* **01** (2019) 132 [arXiv:1810.10017] [INSPIRE].

[26] A. Greljo, J. Martin Camalich and J.D. Ruiz-Álvarez, *Mono-τ signatures at the LHC constrain explanations of B-decay anomalies*, *Phys. Rev. Lett.* **122** (2019) 131803 [arXiv:1811.07920] [INSPIRE].

[27] M.J. Baker, J. Fuentes-Martín, G. Isidori and M. König, *High-p_T signatures in vector-leptoquark models*, *Eur. Phys. J.* **C 79** (2019) 334 [arXiv:1901.10480] [INSPIRE].

[28] L. Di Luzio, A. Greljo and M. Nardecchia, *Gauge leptoquark as the origin of B-physics anomalies*, *Phys. Rev.* **D 96** (2017) 115011 [arXiv:1708.08450] [INSPIRE].

[29] N. Assad, B. Fornal and B. Grinstein, *Baryon number and lepton universality violation in leptoquark and diquark models*, *Phys. Lett.* **B 777** (2018) 324 [arXiv:1708.06350] [INSPIRE].

[30] L. Calibbi, A. Crivellin and T. Li, *Model of vector leptoquarks in view of the B-physics anomalies*, *Phys. Rev.* **D 98** (2018) 115002 [arXiv:1709.00692] [INSPIRE].

[31] M. Bordone, C. Cornella, J. Fuentes-Martín and G. Isidori, *A three-site gauge model for flavor hierarchies and flavor anomalies*, *Phys. Lett.* **B 779** (2018) 317 [arXiv:1712.01368] [INSPIRE].

[32] M. Bordone, C. Cornella, J. Fuentes-Martín and G. Isidori, *Low-energy signatures of the* PS^3 *model: from B-physics anomalies to LFV*, *JHEP* **10** (2018) 148 [arXiv:1805.09328] [INSPIRE].

[33] R. Barbieri and A. Tesi, *B-decay anomalies in Pati-Salam* SU(4), *Eur. Phys. J.* **C 78** (2018) 193 [arXiv:1712.06844] [INSPIRE].

[34] L. Di Luzio, J. Fuentes-Martín, A. Greljo, M. Nardecchia and S. Renner, *Maximal flavour violation: a Cabibbo mechanism for leptoquarks*, *JHEP* **11** (2018) 081 [arXiv:1808.00942] [INSPIRE].

[35] D. Marzocca, *Addressing the B-physics anomalies in a fundamental composite Higgs model*, *JHEP* **07** (2018) 121 [arXiv:1803.10972] [INSPIRE].

[36] D. Bečirević, I. Doršner, S. Fajfer, N. Košnik, D.A. Faroughy and O. Sumensari, *Scalar leptoquarks from grand unified theories to accommodate the B-physics anomalies*, *Phys. Rev.* **D 98** (2018) 055003 [arXiv:1806.05689] [INSPIRE].

[37] A. Greljo and B.A. Stefanek, *Third family quark-lepton unification at the TeV scale*, *Phys. Lett.* **B 782** (2018) 131 [arXiv:1802.04274] [INSPIRE].

[38] M. Blanke and A. Crivellin, *B meson anomalies in a Pati-Salam model within the Randall-Sundrum background*, *Phys. Rev. Lett.* **121** (2018) 011801 [arXiv:1801.07256] [INSPIRE].

JHEP07(2019)168

[39] B. Fornal, S.A. Gadam and B. Grinstein, *Left-right* SU(4) *vector leptoquark model for flavor anomalies*, *Phys. Rev.* **D 99** (2019) 055025 [arXiv:1812.01603] [INSPIRE].

[40] W. Altmannshofer, P.S. Bhupal Dev and A. Soni, $R_{D^{(*)}}$ *anomaly: a possible hint for natural supersymmetry with R-parity violation*, *Phys. Rev.* **D 96** (2017) 095010 [arXiv:1704.06659] [INSPIRE].

[41] S. Trifinopoulos, *Revisiting R-parity violating interactions as an explanation of the B-physics anomalies*, *Eur. Phys. J.* **C 78** (2018) 803 [arXiv:1807.01638] [INSPIRE].

[42] T. Faber, M. Hudec, M. Malinský, P. Meinzinger, W. Porod and F. Staub, *A unified leptoquark model confronted with lepton non-universality in B-meson decays*, *Phys. Lett.* **B 787** (2018) 159 [arXiv:1808.05511] [INSPIRE].

[43] D. Buttazzo, A. Greljo, G. Isidori and D. Marzocca, *B-physics anomalies: a guide to combined explanations*, *JHEP* **11** (2017) 044 [arXiv:1706.07808] [INSPIRE].

[44] B. Bhattacharya, A. Datta, J.-P. Guévin, D. London and R. Watanabe, *Simultaneous explanation of the* R_K *and* $R_{D^{(*)}}$ *puzzles: a model analysis*, *JHEP* **01** (2017) 015 [arXiv:1609.09078] [INSPIRE].

[45] A. Angelescu, D. Bečirević, D.A. Faroughy and O. Sumensari, *Closing the window on single leptoquark solutions to the B-physics anomalies*, *JHEP* **10** (2018) 183 [arXiv:1808.08179] [INSPIRE].

[46] J. Kumar, D. London and R. Watanabe, *Combined explanations of the* $b \to s\mu^+\mu^-$ *and* $b \to c\tau^-\bar{\nu}$ *anomalies: a general model analysis*, *Phys. Rev.* **D 99** (2019) 015007 [arXiv:1806.07403] [INSPIRE].

[47] J. Aebischer, W. Altmannshofer, D. Guadagnoli, M. Reboud, P. Stangl and D.M. Straub, *B-decay discrepancies after Moriond* 2019, arXiv:1903.10434 [INSPIRE].

[48] M. Algueró et al., *Emerging patterns of new physics with and without lepton flavour universal contributions*, arXiv:1903.09578 [INSPIRE].

[49] M. Ciuchini et al., *New physics in* $b \to s\ell^+\ell^-$ *confronts new data on lepton universality*, arXiv:1903.09632 [INSPIRE].

[50] A. Datta, J. Kumar and D. London, *The B anomalies and new physics in* $b \to se^+e^-$, arXiv:1903.10086 [INSPIRE].

[51] A. Azatov, D. Barducci, D. Ghosh, D. Marzocca and L. Ubaldi, *Combined explanations of B-physics anomalies: the sterile neutrino solution*, *JHEP* **10** (2018) 092 [arXiv:1807.10745] [INSPIRE].

[52] D.J. Robinson, B. Shakya and J. Zupan, *Right-handed neutrinos and* $R(D^{(*)})$, *JHEP* **02** (2019) 119 [arXiv:1807.04753] [INSPIRE].

[53] F. Feruglio, P. Paradisi and O. Sumensari, *Implications of scalar and tensor explanations of* $R_{D^{(*)}}$, *JHEP* **11** (2018) 191 [arXiv:1806.10155] [INSPIRE].

[54] S. Fajfer, J.F. Kamenik and I. Nisandzic, *On the* $B \to D^*\tau\bar{\nu}_\tau$ *sensitivity to new physics*, *Phys. Rev.* **D 85** (2012) 094025 [arXiv:1203.2654] [INSPIRE].

[55] M. González-Alonso, J. Martin Camalich and K. Mimouni, *Renormalization-group evolution of new physics contributions to (semi)leptonic meson decays*, *Phys. Lett.* **B 772** (2017) 777 [arXiv:1706.00410] [INSPIRE].

[56] A. Celis, J. Fuentes-Martin, A. Vicente and J. Virto, *DsixTools: the Standard Model effective field theory toolkit*, *Eur. Phys. J.* **C 77** (2017) 405 [arXiv:1704.04504] [INSPIRE].

JHEP07(2019)168

[57] J. Aebischer, J. Kumar and D.M. Straub, *Wilson: a python package for the running and matching of Wilson coefficients above and below the electroweak scale*, *Eur. Phys. J.* **C 78** (2018) 1026 [arXiv:1804.05033] [INSPIRE].

[58] A.G. Akeroyd and C.-H. Chen, *Constraint on the branching ratio of $B_c \to \tau\bar{\nu}$ from LEP1 and consequences for $R(D^{(*)})$ anomaly*, *Phys. Rev.* **D 96** (2017) 075011 [arXiv:1708.04072] [INSPIRE].

[59] R. Alonso, B. Grinstein and J. Martin Camalich, *Lifetime of B_c^- constrains explanations for anomalies in $B \to D^{(*)}\tau\nu$*, *Phys. Rev. Lett.* **118** (2017) 081802 [arXiv:1611.06676] [INSPIRE].

[60] HFLAV collaboration, *Averages of b-hadron, c-hadron and τ-lepton properties as of summer* 2016, *Eur. Phys. J.* **C 77** (2017) 895 [arXiv:1612.07233] [INSPIRE].

[61] A. Celis, J. Fuentes-Martin, A. Vicente and J. Virto, *Gauge-invariant implications of the LHCb measurements on lepton-flavor nonuniversality*, *Phys. Rev.* **D 96** (2017) 035026 [arXiv:1704.05672] [INSPIRE].

[62] B. Capdevila, A. Crivellin, S. Descotes-Genon, J. Matias and J. Virto, *Patterns of new physics in $b \to s\ell^+\ell^-$ transitions in the light of recent data*, *JHEP* **01** (2018) 093 [arXiv:1704.05340] [INSPIRE].

[63] A. Crivellin, C. Greub, D. Müller and F. Saturnino, *Importance of loop effects in explaining the accumulated evidence for new physics in B decays with a vector leptoquark*, *Phys. Rev. Lett.* **122** (2019) 011805 [arXiv:1807.02068] [INSPIRE].

[64] M. Algueró, B. Capdevila, S. Descotes-Genon, P. Masjuan and J. Matias, *Are we overlooking lepton flavour universal new physics in $b \to s\ell\ell$?*, *Phys. Rev.* **D 99** (2019) 075017 [arXiv:1809.08447] [INSPIRE].

[65] S. Descotes-Genon, L. Hofer, J. Matias and J. Virto, *Global analysis of $b \to s\ell\ell$ anomalies*, *JHEP* **06** (2016) 092 [arXiv:1510.04239] [INSPIRE].

[66] HPQCD collaboration, *Rare decay $B \to K\ell^+\ell^-$ form factors from lattice QCD*, *Phys. Rev.* **D 88** (2013) 054509 [*Erratum ibid.* **D 88** (2013) 079901] [arXiv:1306.2384] [INSPIRE].

[67] LHCb collaboration, *Search for the lepton-flavour-violating decays $B_s^0 \to \tau^\pm\mu^\mp$ and $B^0 \to \tau^\pm\mu^\mp$*, arXiv:1905.06614 [INSPIRE].

[68] F. Feruglio, P. Paradisi and A. Pattori, *Revisiting lepton flavor universality in B decays*, *Phys. Rev. Lett.* **118** (2017) 011801 [arXiv:1606.00524] [INSPIRE].

[69] F. Feruglio, P. Paradisi and A. Pattori, *On the importance of electroweak corrections for B anomalies*, *JHEP* **09** (2017) 061 [arXiv:1705.00929] [INSPIRE].

[70] C. Cornella, F. Feruglio and P. Paradisi, *Low-energy effects of lepton flavour universality violation*, *JHEP* **11** (2018) 012 [arXiv:1803.00945] [INSPIRE].

[71] HFLAV collaboration, *Average of $R(D)$ and $R(D^{*+})$ for Spring* 2019 *webpage*, https://hflav-eos.web.cern.ch/hflav-eos/semi/spring19/html/RDsDsstar/RDRDs.html.

[72] D. Bigi and P. Gambino, *Revisiting $B \to D\ell\nu$*, *Phys. Rev.* **D 94** (2016) 094008 [arXiv:1606.08030] [INSPIRE].

[73] F.U. Bernlochner, Z. Ligeti, M. Papucci and D.J. Robinson, *Combined analysis of semileptonic B decays to D and D^*: $R(D^{(*)})$, $|V_{cb}|$ and new physics*, *Phys. Rev.* **D 95** (2017) 115008 [*Erratum ibid.* **D 97** (2018) 059902] [arXiv:1703.05330] [INSPIRE].

JHEP07(2019)168

[74] S. Jaiswal, S. Nandi and S.K. Patra, *Extraction of $|V_{cb}|$ from $B \to D^{(*)}\ell\nu_\ell$ and the Standard Model predictions of $R(D^{(*)})$*, *JHEP* **12** (2017) 060 [arXiv:1707.09977] [INSPIRE].

[75] D. Bigi, P. Gambino and S. Schacht, *$R(D^*)$, $|V_{cb}|$ and the heavy quark symmetry relations between form factors*, *JHEP* **11** (2017) 061 [arXiv:1707.09509] [INSPIRE].

[76] Particle Data Group collaboration, *Review of particle physics*, *Phys. Rev.* **D 98** (2018) 030001 [INSPIRE].

[77] UTfit collaboration, *Latest results for the unitary triangle fit from the UTfit collaboration*, PoS(CKM2016)096 (2017) [INSPIRE].

[78] LHCb collaboration, *Search for the decays $B_s^0 \to \tau^+\tau^-$ and $B^0 \to \tau^+\tau^-$*, *Phys. Rev. Lett.* **118** (2017) 251802 [arXiv:1703.02508] [INSPIRE].

[79] C. Bobeth, M. Gorbahn, T. Hermann, M. Misiak, E. Stamou and M. Steinhauser, *$B_{s,d} \to l^+l^-$ in the Standard Model with reduced theoretical uncertainty*, *Phys. Rev. Lett.* **112** (2014) 101801 [arXiv:1311.0903] [INSPIRE].

[80] BaBar collaboration, *Search for $B^+ \to K^+\tau^+\tau^-$ at the BaBar experiment*, *Phys. Rev. Lett.* **118** (2017) 031802 [arXiv:1605.09637] [INSPIRE].

[81] BaBar collaboration, *A search for the decay modes $B^\pm \to h^\pm\tau^\pm l$*, *Phys. Rev.* **D 86** (2012) 012004 [arXiv:1204.2852] [INSPIRE].

[82] Belle collaboration, *Search for lepton-flavor-violating tau decays into a lepton and a vector meson*, *Phys. Lett.* **B 699** (2011) 251 [arXiv:1101.0755] [INSPIRE].

[83] S. Descotes-Genon, A. Falkowski, M. Fedele, M. González-Alonso and J. Virto, *The CKM parameters in the SMEFT*, *JHEP* **05** (2019) 172 [arXiv:1812.08163] [INSPIRE].

[84] ATLAS collaboration, *Search for additional heavy neutral Higgs and gauge bosons in the ditau final state produced in 36 fb^{-1} of pp collisions at $\sqrt{s} = 13$ TeV with the ATLAS detector*, *JHEP* **01** (2018) 055 [arXiv:1709.07242] [INSPIRE].

[85] CMS collaboration, *Search for heavy neutrinos and third-generation leptoquarks in hadronic states of two τ leptons and two jets in proton-proton collisions at $\sqrt{s} = 13$ TeV*, *JHEP* **03** (2019) 170 [arXiv:1811.00806] [INSPIRE].

[86] H. Georgi and Y. Nakai, *Diphoton resonance from a new strong force*, *Phys. Rev.* **D 94** (2016) 075005 [arXiv:1606.05865] [INSPIRE].

[87] P. Fileviez Perez and M.B. Wise, *Low scale quark-lepton unification*, *Phys. Rev.* **D 88** (2013) 057703 [arXiv:1307.6213] [INSPIRE].

[88] R. Barbieri, G. Isidori, J. Jones-Perez, P. Lodone and D.M. Straub, U(2) *and minimal flavour violation in supersymmetry*, *Eur. Phys. J.* **C 71** (2011) 1725 [arXiv:1105.2296] [INSPIRE].

[89] T. Inami and C.S. Lim, *Effects of superheavy quarks and leptons in low-energy weak processes $K_L \to \mu^+\mu^-$, $K^+ \to \pi^+\nu\bar{\nu}$ and $K^0 \leftrightarrow \bar{K}^0$*, *Prog. Theor. Phys.* **65** (1981) 297 [*Erratum ibid.* **65** (1981) 1772] [INSPIRE].

[90] S.L. Glashow, J. Iliopoulos and L. Maiani, *Weak interactions with lepton-hadron symmetry*, *Phys. Rev.* **D 2** (1970) 1285 [INSPIRE].

[91] M.K. Gaillard and B.W. Lee, *Rare decay modes of the K-mesons in gauge theories*, *Phys. Rev.* **D 10** (1974) 897 [INSPIRE].

[92] L. Silvestrini, *Flavour constraints on NP*, La Thuile 2018, (2018).

JHEP07(2019)168

[93] N. Carrasco et al., D^0-$\bar{D}^0$ *mixing in the Standard Model and beyond from* $N_f = 2$ *twisted mass QCD*, *Phys. Rev.* **D 90** (2014) 014502 [arXiv:1403.7302] [INSPIRE].

[94] X.-G. He, J. Tandean and G. Valencia, *Penguin and box diagrams in unitary gauge*, *Eur. Phys. J.* **C 64** (2009) 681 [arXiv:0909.3638] [INSPIRE].

[95] M. König, M. Neubert and D.M. Straub, *Dipole operator constraints on composite Higgs models*, *Eur. Phys. J.* **C 74** (2014) 2945 [arXiv:1403.2756] [INSPIRE].

[96] A. Alloul, N.D. Christensen, C. Degrande, C. Duhr and B. Fuks, *FeynRules* 2.0 — *a complete toolbox for tree-level phenomenology*, *Comput. Phys. Commun.* **185** (2014) 2250 [arXiv:1310.1921] [INSPIRE].

[97] J. Alwall et al., *The automated computation of tree-level and next-to-leading order differential cross sections and their matching to parton shower simulations*, *JHEP* **07** (2014) 079 [arXiv:1405.0301] [INSPIRE].

[98] ATLAS collaboration, *Combination of the searches for pair-produced vector-like partners of the third-generation quarks at* $\sqrt{s} = 13$ *TeV with the ATLAS detector*, *Phys. Rev. Lett.* **121** (2018) 211801 [arXiv:1808.02343] [INSPIRE].

[99] CMS collaboration, *Search for vector-like leptons in multilepton final states in pp collisions at* $\sqrt{s} = 13$ *TeV*, CMS-PAS-EXO-18-005, CERN, Geneva, Switzerland (2018).

[100] ATLAS collaboration, *Search for supersymmetry in final states with two same-sign or three leptons and jets using* $36\,fb^{-1}$ *of* $\sqrt{s} = 13$ *TeV pp collision data with the ATLAS detector*, *JHEP* **09** (2017) 084 [arXiv:1706.03731] [INSPIRE].

[101] D. Bečirević and O. Sumensari, *A leptoquark model to accommodate* $R_K^{\rm exp} < R_K^{\rm SM}$ *and* $R_{K^*}^{\rm exp} < R_{K^*}^{\rm SM}$, *JHEP* **08** (2017) 104 [arXiv:1704.05835] [INSPIRE].

[102] D. Bečirević, S. Fajfer, N. Košnik and O. Sumensari, *Leptoquark model to explain the B-physics anomalies,* R_K *and* R_D, *Phys. Rev.* **D 94** (2016) 115021 [arXiv:1608.08501] [INSPIRE].

[103] Y. Bai and B.A. Dobrescu, *Collider tests of the renormalizable Coloron model*, *JHEP* **04** (2018) 114 [arXiv:1802.03005] [INSPIRE].

[104] T. Faber et al., *Collider phenomenology of a unified leptoquark model*, arXiv:1812.07592 [INSPIRE].

[105] B. Grinstein, R.P. Springer and M.B. Wise, *Effective Hamiltonian for weak radiative B meson decay*, *Phys. Lett.* **B 202** (1988) 138 [INSPIRE].

[106] G. Buchalla, A.J. Buras and M.E. Lautenbacher, *Weak decays beyond leading logarithms*, *Rev. Mod. Phys.* **68** (1996) 1125 [hep-ph/9512380] [INSPIRE].

[107] A.J. Buras, *Weak Hamiltonian, CP-violation and rare decays*, in *Probing the Standard Model of particle interactions. Proceedings, Summer School in Theoretical Physics, NATO Advanced Study Institute,* $68^{\rm th}$ *session*, Les Houches, France, 28 July–5 September 1997, pg. 281 [hep-ph/9806471] [INSPIRE].

JHEP07(2019)168